Article

Not peer-reviewed version

On the determination of elastic properties of single-walled nitride nanotubes using numerical simulation

Nataliya A. Sakharova *, André F.G. Pereira, Jorge M. Antunes, Bruno M. Chaparro, Tomás G. Parreira, José V. Fernandes

Posted Date: 9 April 2024

doi: 10.20944/preprints202404.0629.v1

Keywords: 13th group element; nitride nanotubes; rigidity; elastic moduli; modelling; numerical simulation.

Article

On the Determination of Elastic Properties of Single-Walled Nitride Nanotubes Using Numerical Simulation

Nataliya A. Sakharova [1,*], André F.G. Pereira [1], Jorge M. Antunes [1,2], Bruno M. Chaparro [2], Tomás G. Parreira [1] and José V. Fernandes [1]

[1] Centre for Mechanical Engineering, Materials and Processes (CEMMPRE) - Advanced Production and Intelligent Systems, Associated Laboratory (ARISE), Department of Mechanical Engineering, University of Coimbra, Rua Luís Reis Santos, Pinhal de Marrocos, 3030-788 Coimbra, Portugal; andre.pereira@uc.pt (A.F.G.P.); jorge.antunes@dem.uc.pt (J.M.A.); tomas.parreira@dem.uc.pt (T.G.P); valdemar.fernandes@dem.uc.pt (J.V.F.)

[2] Abrantes High School of Technology, Polytechnic Institute of Tomar, Quinta do Contador, Estrada da Serra, 2300-313 Tomar, Portugal; bruno.chaparro@ipt.pt (B.M.C.)

* Correspondence: nataliya.sakharova@dem.uc.pt (N.A.S.); Tel.: +351-239-790-700

Abstract: In the recent years, tubular nanostructures have been related with immense advances in various fields of science and technology. Considerable research efforts have been centered on the theoretical prediction and manufacturing of non-carbon nanotubes (NTs), which meet modern requirements for the developing of novel devices and systems. In this context, diatomic inorganic nanotubes formed by atoms of elements from the 13th group of the periodic table (B, Al, Ga, In, Tl) and nitrogen (N), have received much research attention. In the present work, the elastic properties of single-walled boron nitride, aluminium nitride, gallium nitride, indium nitride and thallium nitride nanotubes were numerically evaluated using the nanoscale continuum modelling approach (also called molecular structural mechanics). The elastic properties (rigidities, surface Young´s and shear moduli, and Poisson´s ratio) of nitride nanotubes are discussed with respect to the bond length of the corresponding diatomic hexagonal lattice. The results obtained contribute to a better understanding of the mechanical response of nitride compound-based nanotubes, covering a broad range from the well-studied boron nitride NTs to the hypothetical thallium nitride NTs.

Keywords: 13th group element; nitride nanotubes; rigidity; elastic moduli; modelling; numerical simulation

1. Introduction

Compounds of elements of the 13th group of the periodic table, such as boron (B), aluminum (Al), gallium (Ga), indium (In) and thallium (Tl), with nitrogen (N), representative of the 15th group, are emerging materials attractive for electronic engineering and light industry. The ability of 13th group-nitrides to form a hexagonal graphene-like lattice [1] allows to expand the area of their upcoming applications and bring to light new perspectives in miniaturization and design of functional devices [2–4]. Hexagonal boron nitride (h-BN) is a high strength electric insulator, comparable to graphene, excellent thermal and chemical stability, and transparency for visible light [5–7]. Such characteristics make h-BN suitable for diverse applications as a dielectric in graphene electronics, components for photovoltaic devices, sensors and bio-detectors. Hexagonal aluminium nitride (h-AlN), gallium nitride (h-GaN) and indium nitride (h-InN), which also exhibit good thermal and chemical stability, are wide gap semiconductors and are able of emitting light in colours green, blue and UV bands [8]. As a result, these hexagonal metal nitrides (AlN, GaN and InN) are in the focus of research attention due to their promising applications in electronics and optoelectronics as solid-state light-emitting devices (LED) and high-speed field-effect transistors (FETs) [1,4,9].

 doi:10.20944/preprints202404.0629.v1

Hexagonal thallium nitride (h-TlN), has a small or even negative band gap [10], pointing out to its semi-metallic nature. This makes h-TlN an appropriate candidate for infrared optical devices [3,11].

One-dimensional (1D) tubular nanostructures, i.e. nanotubes (NTs), made up from hexagonal BN, AlN, GaN, InN and TlN monolayers, are expected to have enhanced properties when compared with their bulk counterparts, envisioning new perspectives in the development of nanoscale electronic and light devices, but not limited to them. For example, boron nitride nanotube has the potential to be used in the smallest co-axial cable, a possibility that was unlocked when carbon nanotube was grown inside it [12]. The high surface to volume ratio of NTs allows suggesting their forthcoming applications for gas absorption and as chemical sensors. The possibility of tuning electronic, thermoelectric, optical and chemical properties of two-dimensional (2D) 13th group-nitride nanostructures through the introducing deformation [1,4,13–17], points to a promising use of their 1D allotropes in the field of strain engineering. In view of abovementioned perspectives, viable applications of boron nitride NTs as biosensors [18], aluminium nitride NTs as gas adsorbents [19] and for drug delivery [20], as well as suitability of gallium nitride NTs for nanoelectromechanical systems (NEMS) [21] were considered.

Most nanotubes based on the 13th group-nitride compounds were by now predicted and synthesized. After the theoretical prediction of the boron nitride nanotube (BNNT) in 1994 [22] and its synthetization in 1995 by Chowdhury and Adhikari [23], who used arc discharge for this end, BN nanotubes with a honeycomb atomic arrangement were successfully manufactured using chemical vapour deposition (CVD) [24,25], ball-milling [26], laser ablation [27] and thermal plasma jet [28]. Unlike BNNTs, progress in synthesizing of AlN, GaN and InN nanotubes is to some extent limited. In 2003, Zhang and Zhang [29] performed a theoretical study on the stability of the geometrical structure of aluminium nitride nanotubes (AlNNTs) and perspectives for their synthesis. It was concluded that the Al and N atoms form a hexagonal graphene-like arrangement, carrying out sp^2 hybridization [29]. Wu et al. [30] synthesized AlNNTs by nitriding reaction, in the same year. The proposed growth method made it possible to obtain faceted AlNNTs with a length of a few micrometers and a hexagonal cross section. Balasubramanian et al. [31] grew AlNNTs by gas-phase condensation using solid–vapour equilibrium. The atomic structure of the resulting AlNNTs consisted of hexagonal rings of Al and N atoms, which adopt sp^2 hybridization. Yin et al. [32] produced C–AlN–C coaxial composite NTs in mass quantity, by resorting to a chemical substitution reaction in a controllable two-step process with the use of multi-walled carbon nanotubes (MWCNTs) as template. The AlNNTs obtained were straight, several micrometers long and had a faceted single-crystalline structure. Stan et al. [33] synthesized faceted AlNNTs with a triangular cross-section through an epitaxial casting process that consisted of the depositing of aluminium nitride onto GaN nanowires, which were subsequently removed by annealing in a hydrogen atmosphere, so that the AlN tubes remained hollow. Finally, one-micrometer-long AlNNTs with hexagonal wurtzite structure were synthesized by Fan et al. [34], who used a thermal process to bend and roll-up the AlN monolayer for this purpose. With regard to gallium nitride nanotubes (GaNNTs), their structural stability and prospects of synthesis were first theoretically investigated in 1999 by Lee et al. [35], basing on density functional theory (DFT) calculations. Then, in 2003 Goldberger et al. [36] prepared single-crystalline GaNNTs with hexagonal cross-section, using an epitaxial casting method and ZnO nanowires as templates. Yin et al. [37] synthesized amorphous GaNNTs of a few micrometers in length by an In-assisted thermal evaporation process. Hu et al. [38] accomplished mass-quantity growth of straight crystalline GaNNTs with lengths up to 80 μm, using a two-stage process based on controllable conversion of amorphous gallium oxide NTs. Hung et al. [39] synthesized uniform arrays of free-standing hexagonal GaNNTs on a GaN template by inductively coupled plasma etching. Liu et al. [40] manufactured single-crystalline hexagonal wurtzite-type GaNNTs based on controllable chemical thermal evaporation process. Jung et al. [41] fabricated long crystalline GaNNTs aided by the metal organic chemical vapour deposition (MOCVD) technique. Concerning indium nitride nanotubes (InNNTs), for the first time in 2004, Yin et al. [42] synthesized straight, high purity, crystalline InNNTs of several-micrometers length in mass quantity by controlled carbonitridation reaction in a vapour-solid (VS) route, using MWCNTs as carbon source to carry out chemical reaction.

 doi:10.20944/preprints202404.0629.v1

Soon after, Sardar et al. [43] produced almost defect-free single-crystalline InNNTs by employing the low-temperature chemical reaction of indium acetate with hexamethyldisilazane (HMDS). At about the same time, the theoretical prediction of the InNNTs with stable honeycomb graphene-like structure was accomplished by Qian et al. [44], who used DFT calculations to this end.

Among the 13th group – nitrides, TlN is the least studied and nanostructures based on this compound have not been synthesized, possibly due to the high toxicity of thallium [2]. Despite the existence of several theoretical works dedicated to the structural stability of 2D TlN nanostructures with planar honeycomb atomic arrangement [45–47] and evaluation of their electronic [3,4] and mechanical [1,47] properties, thallium nitride nanotubes (TlNNTs) have not yet been predicted. The structural similarity of h-TlN with other representatives of the 13th group-nitrides suggests that TlNNTs will possibly be modelled and synthesized in the future. The inclusion of these hypothetical nanotubes in the current study envisages expanding the range of the potential applications of 13th group-nitride NTs and meets the requirements for the search of new materials for innovative nanodevices.

The mechanical stability of nanotubes and the knowledge on their mechanical behaviour are crucial for current and forthcoming applications involving NTs, as well as for the design of materials and instrument. It is worth noting that strain engineering is efficient to customize the functional properties of nanomaterials. From this point of view, the evaluation of the mechanical properties of the 13th group-nitride NTs gains the outmost importance.

The study of the mechanical behaviour of non-carbon nanotubes (N-CNTs), whose representatives are those based on nitride compounds, has been performed mostly theoretically, aided by analytical and numerical procedures, since experimental techniques for nanomaterials characterization are expensive and highly resource-consuming. As reported by Antunes et al. [48], the mechanical behaviour of N-CNTs can be characterized using three categories of theoretical methods, viz.: the atomistic approach, embracing ab initio and molecular dynamics (MD); the continuum mechanics (CM) approach; and the nanoscale continuum modelling (NCM) or molecular structural mechanics (MSM) approach. Amongst 13th group-nitride nanotubes, BNNTs have received the most research attention to date [48,49].

Referring to the atomistic approach, Kochaev [50] evaluated the surface Young's modulus (product of Young's modulus and nanotube wall thickness) and Poisson´s ratio of BNNTs, AlNNTs and GaNNTs, making use of ab initio simulation. Hao et al. [51] studied size-dependent mechanical behaviour of the AlNNTs and evaluated their Young's modulus employing ab initio DFT calculations coupled with linear combination of atomic orbitals (LCAO). Fabris et al. [52] used the same method to calculate the Young's modulus of GaNNTs. Current studies, involving MD, rely on analytical or empirical potential functions to describe the interactions between atoms in the hexagonal diatomic lattice. The second-generation reactive empirical bond order (REBO) potential was used by Kumar et al. [53] in their MD simulation study to evaluate the Young´s and shear moduli, and Poisson´s ratio of BNNTs, AlNNTs and GaNNTs. Jeng et al. [54] adopted MD simulation with Tersoff many-body potential to assess the mechanical properties of GaNNTs under tension, including their Young´s modulus. Xiong and Tian [55] studied the torsional properties of BNNTs, making use of MD simulation with Tersoff potential and calculated BNNTs the shear modulus. Tao et al. [56] used MD with Tersoff–Brenner (TB) potential to calculate the Young's modulus of BNNTs. The Stilliger-Weber (S-W) potential was employed to describe the interactions between Ga and N atoms by Xu et al. [57] in their MD simulation study for evaluating the Young´s modulus of single-crystalline GaNNTs. Santosh et al. [58] with the aim of calculating the BNNTs Young's and shear moduli, implemented the force - constant approach for describing the B - N interactions under MD simulation. Le [59], based on MD simulations coupled with dimensional analysis, derived analytical expressions for the Young's modulus of the BNNTs.

With regard to the CM approach, where the nanotube is modelled as a continuum structure, Oh [60] employed a continuum lattice (CL) analytical thermodynamic method, in combination with the TB potential to calculate the Young's modulus and Poisson's ratio of BNNTs.

 doi:10.20944/preprints202404.0629.v1

In the NCM/MSM approach, the bonds between two atoms in the diatomic lattice are modelled as elastic elements (e.g., beams or springs), thus basing on the connection between NTs molecular structure and solid mechanics. In two their works Sakharova et al. [49,61] used the beam element to represent interatomic bonding within the framework of the NCM/MSM approach to evaluate Young´s and shear moduli, and the Poisson´s ratio of BNNTs [49] and InNNTs [61]. The latter, to our knowledge, is the only study devoted to the elastic properties of InNNTs. Employing the NCM/MSM approach combined with Euler beam model, Yan et al. [62] calculated the Young´s and shear moduli of BNNTs resorting to longitudinal and torsional free-vibrations of nanotubes. Genoese et al. [63] evaluated the surface Young´s and shear moduli of BNNTs, based on a link between the "stick-and-spring" (NCM/MSM) and the Donnell thin shell continuum models (CM). Jiang and Guo [64] also used the "stick-and-spring" model to derive analytical solutions for the surface Young's modulus and Poisson´s ratio of BNNTs, AlNNTs and GaNNTs. With the exception of BNNTs, studies for mechanical characterization of NTs based on other nitrides of the 13th group –are limited (AlNNTs, GaNNTs), infrequent (InNNTs) or absent (TlNNTs). Lack of systematized investigation of the mechanical response of the nanotubes formed by nitride compounds is also noticeable.

The objective of this work is to perform a systematic comparative study on the evaluation of the elastic properties (surface Young´s and shear moduli, and Poisson´s ratio) of single-walled nanotubes made of boron nitride, aluminium nitride, gallium nitride, indium nitride and thallium nitride (SWBNNTs, SWAlNNTs, SWGaNNTs, SWInNNTs and SWTlNNTs) in a wide range of chiral indices and diameters greater than 1.25 nm. To this end, a three-dimensional finite element (FE) model was built within the scope of the NCM/MSM approach to assess three rigidities (tensile, bending and torsional) and then calculate the surface Young´s and shear moduli and Poisson´s ratio of the 13th group – nitride nanotubes. In view of the lack of information on the value of nanotube wall thickness for nitride NTs, except in the case of SWBNNTs, the surface elastic moduli (the product of the respective elastic modulus by the NT wall thickness) were chosen for this analysis. The present work aims to improve the understanding of the mechanical response of the nitride nanotubes, which group materials with insulator, semiconductor and semi-metallic properties.

2. Materials and Methods

2.1. Atomic Structure of 13th Group Element - Nitride Nanotubes

Boron nitride, aluminium nitride, gallium nitride, indium nitride and thallium nitride sheets have a hexagonal lattice, where the atom that is part of the 13th group of the periodic table (now designated A13), such as boron (B), aluminium (Al), gallium (Ga), indium (In) or thallium (Tl) form with nitrogen (N) a honeycomb structure with planar geometry [1,65], as shown in Figure 1 for the case of the GaN nanosheet. The honeycomb atomic arrangement is defined by the chiral vector, $\mathbf{C_h}$, and the chiral angle, θ, expressed as follows, respectively:

$$\mathbf{C_h}=n\boldsymbol{a_1}+m\boldsymbol{a_2}, \tag{1}$$

$$\theta=\sin^{-1}\frac{\sqrt{3}}{2}\frac{m}{\sqrt{n^2+nm+m^2}}, \tag{2}$$

where n and m are the chiral indices, both having integers values; $\boldsymbol{a_1}$ and $\boldsymbol{a_2}$ are the unit vectors of the diatomic hexagonal lattice. The length of the unit vector $\boldsymbol{a}$ is calculated by $a=\sqrt{3}a_{A13\text{-}N}$, where $a_{A13\text{-}N}$ is the equilibrium bond length. As can be seen in Table 1, where the bond lengths of nitride NTs available in the literature are presented, there is no conformity about the $a_{A13\text{-}N}$ values.

Preprints.org (www.preprints.org) | NOT PEER-REVIEWED | Posted: 9 April 2024 doi:10.20944/preprints202404.0629.v1

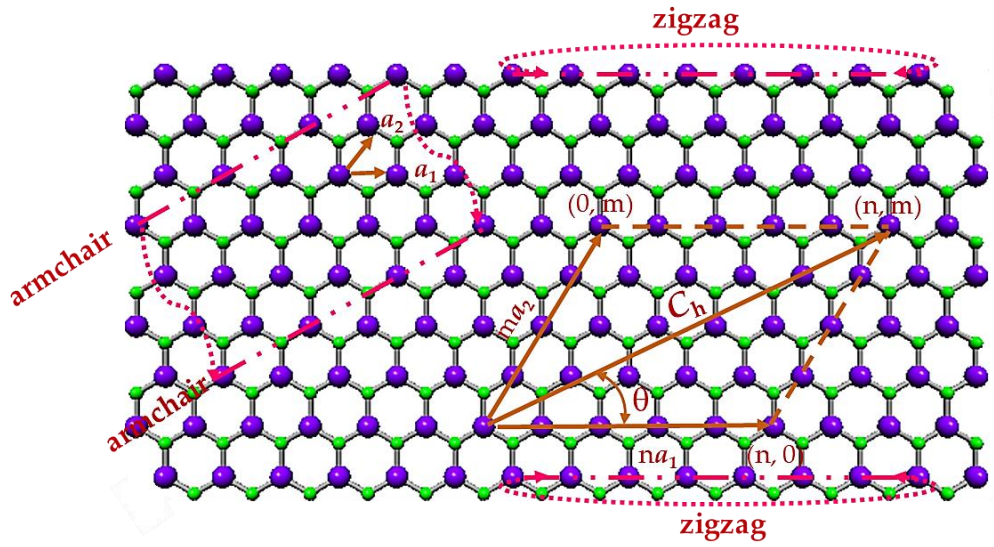

Figure 1. GaN hexagonal nanosheet with designations of the chiral indices, n and m, chiral vector, $\mathbf{C_h}$, chiral angle, θ, and the schematic to roll up armchair and zigzag NTs geometries. Ga atoms are depicted in purple; N atoms in green.

Table 1. Bond length values of 13th group element - nitride nanostructures available in the literature.

	BN	AlN	GaN	InN	TlN
$a_{A13\text{-}N}$, **nm**	0.1446 [53] 0.1447 [66] 0.145 [65] 0.147 [50] 0.151 [67] 0.153 [68]	0.177 [50] 0.179 [65] 0.1805 [1] 0.185 [69] 0.1856 [53] 0.193 [70] 0.195 [71]	0.175 [72] 0.184 [50] 0.185 [65] 0.1852 [1] 0.186 [69] 0.1863 [53] 0.194 [70]	0.203 [44] 0.206 [65] 0.2074 [1]	0.2154 [1] 0.224 [46] 0.230 [4]

Single-walled nitride NTs are cylinders, which are formed by rolling up the respective A13-N nanosheet with a honeycomb atomic arrangement, varying the chiral angle, θ, in the range $0° \le \theta \le 30°$. The diameter of resulting nanotube, D_n, is given by:

$$D_n = \frac{a_{A13\text{-}N}\sqrt{3(n^2+nm+m^2)}}{\pi}, \quad (3)$$

where n and m are the chiral indices and $a_{A13\text{-}N}$ is the equilibrium bond length of the diatomic nanostructure based on the nitride compounds under study.

Three main symmetry groups of NTs are defined based on the value of θ, such as: zigzag (n, 0) NTs with $\theta = 0°$ (m = 0); chiral (n, m) NTs with $0° < \theta < 30°$ ($n \neq m \neq 0$); armchair (n, n) NTs with $\theta = 30°$ (n = m). The two configurations, limiting the range of θ, viz. zigzag (n, 0) and armchair (n, n) (see, Figure 1) are called non-chiral nanotubes.

Non-chiral (zigzag and armchair) and chiral SWBNNTs, SWAlNNTs, SWGaNNTs, SWInNNTs and SWTlNNTs, with the same chiral indices (n, m) for each symmetry group, are represented schematically in Figure 2.

SWBNNTs **SWAlNNTs** **SWGaNNTs** **SWInNNTs** **SWTlNNTs**

 doi:10.20944/preprints202404.0629.v1

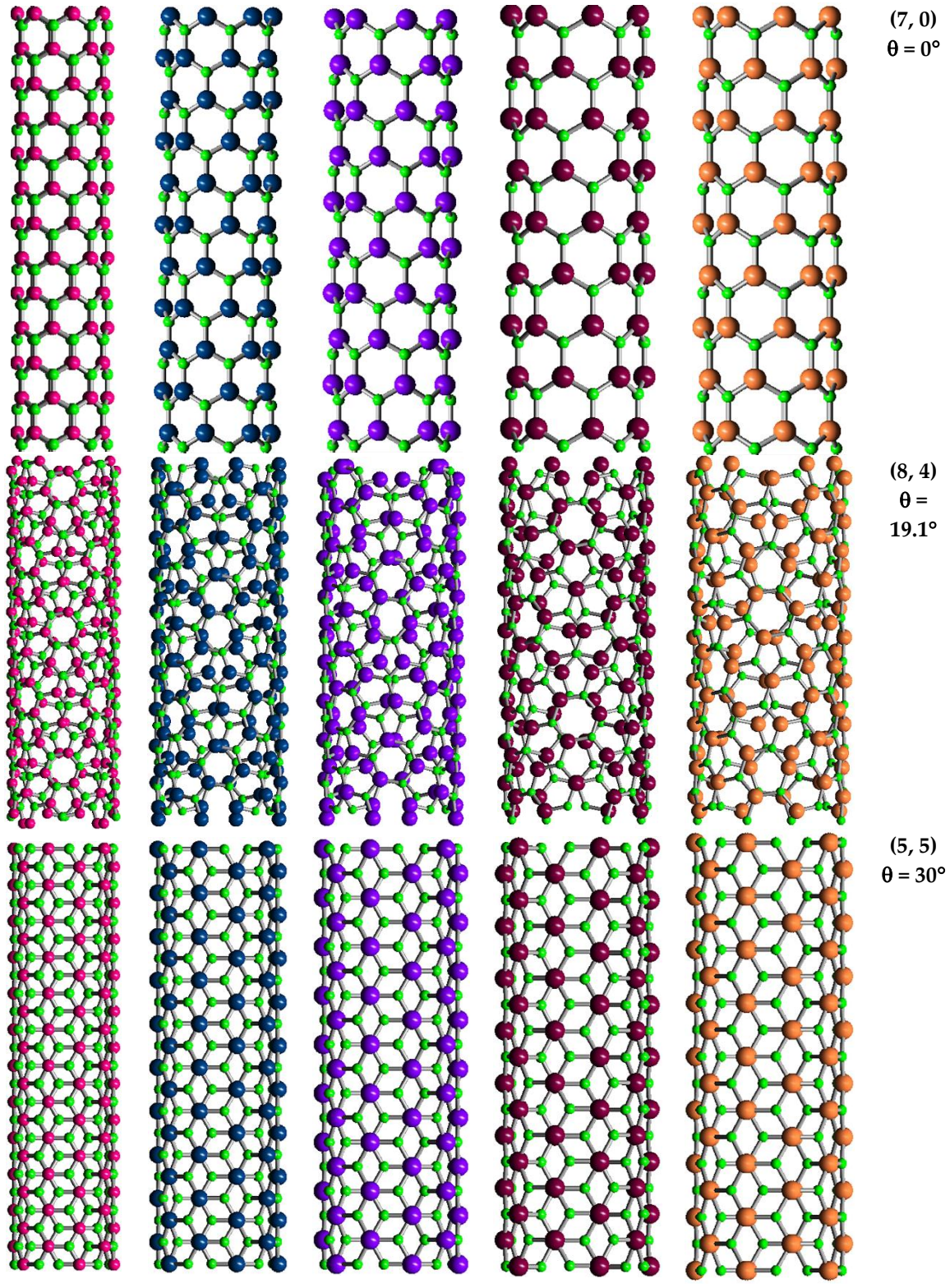

Figure 2. Configurations of (7, 0) zigzag, (8, 4) chiral and (5, 5) armchair of SWBNNTs, SWAlNNTs, SWGaNNTs, SWInNNTs and SWTlNNTs, obtained using the software Nanotube Modeler©. N atoms are depicted in green, B atoms are in bright pink, Al atoms are in blue, Ga atoms are in purple, In atoms are in dark red and Tl atoms are in pale orange.

2.2. Geometrical Characteristics and Finite Element Modeling of the Elastic Behaviour of SWBNNTs, SWAlNNTs, SWGaNNTs, SWInNNTs and SWTlNNTs

 doi:10.20944/preprints202404.0629.v1

The geometric characteristics of SWBNNTs, SWAlNNTs, SWGaNNTs, SWInNNTs and SWTlNNTs of three main configurations, armchair (θ = 30°), zigzag (θ = 0°) and chiral (θ = 19.1° family, which is consistent with the biggest number of NTs), used in the finite element analysis (FEA), are shown in Table 2. The chiral indices of the NTs were chosen to obtain structures with comparable diameters. To guarantee the mechanical response of the NTs regardless of the nanotube length, the length of the NTs was chosen nearly 30 times bigger than the diameter of the NTs [49].

Table 2. Chiral indices (n, m) and diameters, D_n, of the SWBNNTs, SWAlNNTs, SWGaNNTs, SWInNNTs and SWTlNNTs.

NT type	SWBNNTs		SWAlNNTs		SWGaNNTs		SWInNNTs		SWTlNNTs	
	(n, m)	D_n, nm*	(n, m)	D_n, nm*	(n, m)	D_n, nm*	(n, m)	D_n, nm	(n, m)	D_n, nm
zigzag, θ = 0°	(16, 0)	1.297	(13, 0)	1.312	(13, 0)	1.398	(12, 0)	1.363	(11, 0)	1.306
	(26, 0)	2.107	(20, 0)	2.018	(19, 0)	2.043	(18, 0)	2.044	(17, 0)	2.019
	(38, 0)	3.080	(29, 0)	2.926	(27, 0)	2.903	(26, 0)	2.953	(25, 0)	2.969
	(43, 0)	3.485	(34, 0)	3.430	(32, 0)	3.440	(30, 0)	3.407	(29, 0)	3.444
	(47, 0)	3.809	(38, 0)	3.834	(36, 0)	3.870	(34, 0)	3.862	(32, 0)	3.800
chiral, θ = 19.1°	(14, 7)	1.501	(10, 5)	1.335	(10, 5)	1.422	(10, 5)	1.502	(10, 5)	1.571
	(20, 10)	2.144	(16, 8)	2.136	(14, 7)	1.991	(14, 7)	2.103	(14, 7)	2.199
	(26, 13)	2.788	(22, 11)	2.936	(20, 10)	2.844	(20, 10)	3.005	(18, 9)	2.828
	(28, 14)	3.002	(26, 13)	3.470	(24, 12)	3.413	(24, 12)	3.606	(22, 11)	3.456
	(32, 16)	3.431	(30, 15)	4.004	(28, 14)	3.982	(26, 13)	3.906	(26, 13)	4.085
armchair, θ = 30°	(10, 10)	1.404	(8, 8)	1.398	(7, 7)	1.303	(7, 7)	1.377	(7, 7)	1.440
	(15, 15)	2.106	(12, 12)	2.097	(11, 11)	2.048	(11, 11)	2.164	(10, 10)	2.057
	(20, 20)	2.807	(17, 17)	2.971	(16, 16)	2.979	(15, 15)	2.951	(14, 14)	2.880
	(25, 25)	3.509	(20, 20)	3.495	(19, 19)	3.538	(18, 18)	3.541	(17, 17)	3.497
	(27, 27)	3.790	(22, 22)	3.845	(21, 21)	3.910	(20, 20)	3.934	(19, 19)	3.908

* The diameters, D_n, of SWBNNTs, SWAlNNTs and SWGaNNTs are calculated adopting the bond lengths $a_{B\text{-}N}$= 0.147 nm, $a_{Al\text{-}N}$= 0.183 nm and $a_{Ga\text{-}N}$= 0.195 nm, respectively as defined by Nanotube Modeler©software; for the SWInNNTs and SWTlNNTs, the bond lengths $a_{In\text{-}N}$= 0.206 nm [65] and $a_{Tl\text{-}N}$= 0.2154 nm [1] were respectively assumed.

The FE meshes of SWBNNTs, SWAlNNTs, SWGaNNTs, SWInNNTs and SWTlNNTs used in FEA were built using the Nanotube Modeler© software. The program database files, acquired from this software, were converted to the format compatible with the ABAQUS® code. The in-house application *InterfaceNanotubes.NM* [49] was used for this purpose. FE meshes for zigzag, chiral and armchair InNNTs are exemplified in Figure 3.

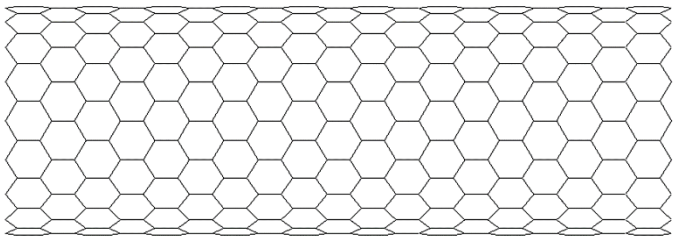

(18, 0)

Preprints.org (www.preprints.org) | NOT PEER-REVIEWED | Posted: 9 April 2024 doi:10.20944/preprints202404.0629.v1

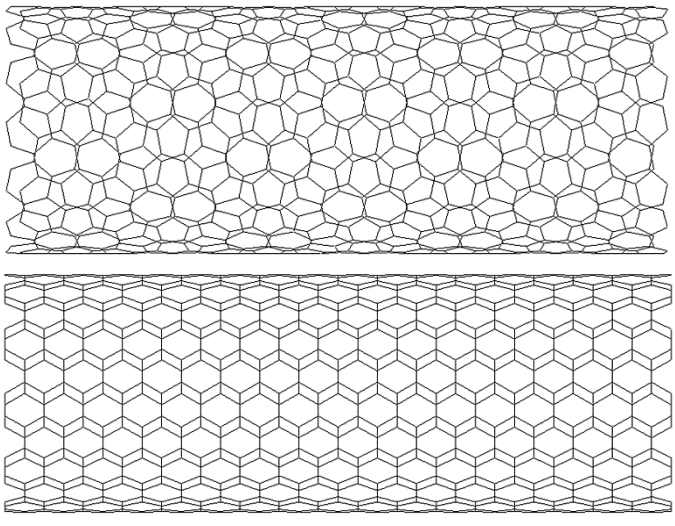

Figure 3. FE meshes of zigzag (18, 0), chiral (14, 7) and armchair (11, 11) InN nanotubes.

The interatomic bonds, A13 – N, of the hexagonal NTs lattice were modelled as equivalent beam elements within the framework of the NCM/MSM approach, which makes use of the connection between the nanotube molecular structure and the equivalent continuum structure. The latter is composed of beam elements and characterised by its tensile, E_bA_b, bending, E_bI_b, and torsional, G_bJ_b, rigidities, which are related to the bond stretching, k_r, bond bending, k_θ, and torsional resistance, k_τ, force field constants, representing the respective molecular structure, through the following expressions [73]:

$$E_bA_b = lk_r,\ E_bI_b = lk_\theta,\ G_bJ_b = lk_\tau, \tag{4}$$

where, $A_b = \pi d^2/4$ is the cross-section area, $I_b = \pi d^4/64$ is the moment of inertia, and $J_b = \pi d^4/32$ is the polar moment of inertia of a circular cross-section beam with diameter d, being l the beam length, equal to the bond length, $a_{A13\text{-}N}$.

Equations (4) allow computing the input parameters for the numerical simulation making use of the k_r, k_θ, and k_τ force field constants. Unlike BNNTs, for which several values of the bond stretching, k_r, and bond bending, k_θ, force constants are available in the literature [49], for the other 13th group elements - nitride NTs, these data are scarce or inexistent. For this reason, in the present study, the k_r and k_θ force field constants were calculated resorting to the method that uses analytical molecular mechanics (MM) expressions for the surface Young's modulus, E_s, and the Poisson's ratio, ν. The values of E_s and ν, in turn, originate from DFT calculations or can be obtained experimentally. Thus, the bond stretching and bond bending force constants are derived by solving the following system of equations [74]:

$$\begin{cases} E_s = \dfrac{4\sqrt{3}k_rk_\theta}{k_r\dfrac{a_{A13\text{-}N}^2}{2}+9k_\theta} \\ \nu = \dfrac{k_ra_{A13\text{-}N}^2-6k_\theta}{k_ra_{A13\text{-}N}^2+18k_\theta}. \end{cases} \tag{5}$$

As a result, the k_r and k_θ force field constants are assessed as follows:

$$k_r = \frac{3E_s}{\sqrt{3}(1-\nu)}, \tag{6}$$

$$k_\theta = \frac{E_sa_{A13\text{-}N}^2}{2\sqrt{3}(1+3\nu)}. \tag{7}$$

Preprints.org (www.preprints.org) | NOT PEER-REVIEWED | Posted: 9 April 2024 doi:10.20944/preprints202404.0629.v1

The parameters $a_{A13\text{-}N}$, E_s and ν, necessary for calculating the bond stretching, k_r, and bond bending, k_θ, force constants (Equations (6) and (7)) together with calculated k_r and k_θ values are presented in Table 3.

With regard to the torsion resistance force constant, k_τ, the value calculated by Ansari et al. [75], based on the relationship of the k_τ constant with the bending rigidity of the BN nanosheet, was adopted for SWBNNTs. For the remaining nitride NTs under study, the k_τ was acquired using DREIDING force field [76], where the torsional behaviour is defined only by the hybridization of the diatomic nanostructure atoms. The values used for k_τ are shown in Table 3.

Table 3. Bond length, surface Young's modulus and Poisson's ratio, and k_r, k_θ and k_τ force field constants for BN, AlN, GaN, InN and TlN nanotubes.

Compound	$a_{A13\text{-}N}$, nm [65]	E_s, nN/nm [65]	ν [65]	k_r, nN/nm	k_θ, nN·nm/rad²	k_τ, nN·nm/rad²
BN	0.145	267	0.21	585	0.994	2.470
AlN	0.179	116	0.46	372	0.451	0.625
GaN	0.185	110	0.48	366	0.445	
InN	0.206	67	0.59	283	0.296	
TlN	0.2154*	34.5*	0.689*	192	0.151	

* Values from Ye and Peng [1].

Finally, based on Equations (4) and the values of k_r, k_θ, and k_τ from Table 3, and taking into account the equality of the bond and beam lengths, $a_{A13\text{-}N} = l$, it is possible to calculate of the input values for the numerical simulation (geometrical and elastic properties of the beams) according to Table 4, together with their respective formulation.

Table 4. Geometrical and elastic properties of beams as input parameters in FE simulations.

Compound	diameter, d, nm	Formulation	Young´s modulus, E_b, GPa	Formulation	Shear modulus, G_b, GPa	Formulation	Poisson´s ratio, ν_b
BN	0.1648	$d = 4\sqrt{\frac{k_\theta}{k_r}}$	3977	$E_b = \frac{k_r^2 l}{4\pi k_\theta}$	4941	$G_b = \frac{k_r^2 k_\tau l}{8\pi k_\theta^2}$	0.21 [65]
AlN	0.1392		4374		3032		0.46 [65]
GaN	0.1395		4437		3113		0.48 [65]
InN	0.1294		4432		4674		0.59 [65]
TlN	0.1120		4200		8712		0.689 [1]

2.3. Elastic Properties of SWBNNTs, SWAlNNTs, SWGaNNTs, SWInNNTs and SWTlNNTs

Firstly, the tensile, EA, bending, EI, and torsional, GJ, rigidities of the 13th group – nitride nanotubes were obtained from the results of the FE analysis, carrying out tensile, bending, and torsion tests using the ABAQUS® FE code (see Figure 4). To perform each abovementioned test, the axial tensile force, F_z, the transverse force, F_y, and the torsional moment, T, were applied to one end of the NT. The boundary conditions applied at the opposed NT end, restricted all degrees of freedom of the nodes involved. In the torsion test, an additional boundary condition was imposed, which consists in preventing the edge nodes from moving in the radial direction, as shown in Figure 4c. Consequently, the tensile, bending and torsion tests made it possible to acquire the axial displacement, u_z, the transverse displacement, u_y, and the twist angle, φ, directly from the FEA. These results are used to calculate the tensile, EA, bending, EI, and torsional, GJ, rigidities of the nitride NTs with the length L_n as follows:

$$EA = \frac{F_z L_n}{u_z}, \tag{8}$$

Preprints.org (www.preprints.org) | NOT PEER-REVIEWED | Posted: 9 April 2024 doi:10.20944/preprints202404.0629.v1

$$EI=\frac{F_y L_n^3}{3u_y}, \quad (9)$$

$$GJ=\frac{TL_n}{\varphi}. \quad (10)$$

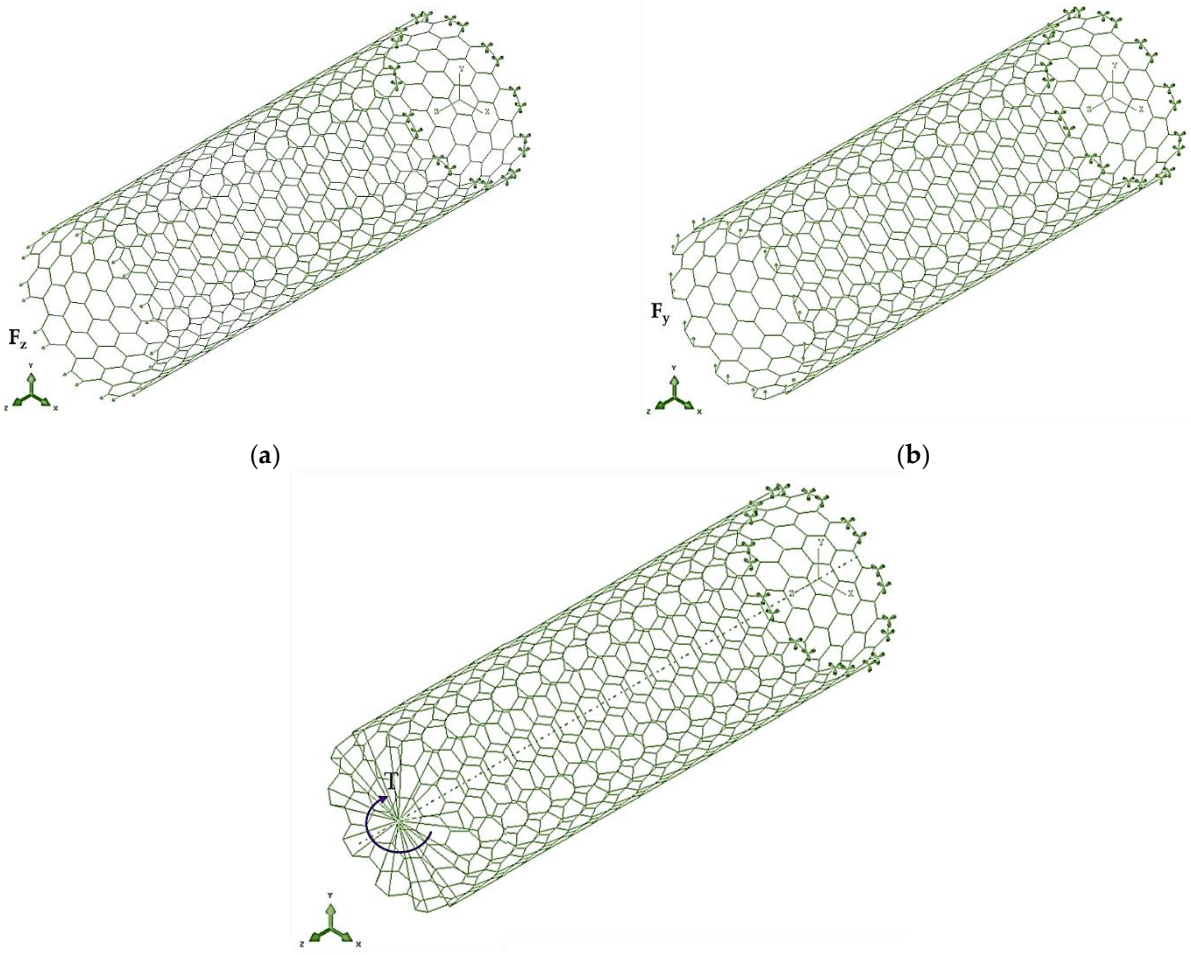

Figure 4. Boundary and loading conditions applied in tests of: (**a**) tension, (**b**) bending and (**c**) torsion, of armchair SWInNNTs.

The tensile, EA, and bending, EI, rigidities from Equations (8) and (9), respectively, are required to assess the Young´s modulus, E, of the nitride NTs as follows [77]:

$$E=\frac{EA}{\pi t_n\sqrt{8\left(\frac{EI}{EA}\right)-t_n^2}}, \quad (11)$$

where t_n is the nanotube wall thickness. The knowledge of the valid value of t_n is not available for most of the 13th group element – nitride NTs, except for BNNTs.

To calculate the shear modulus, G, the torsional rigidity, GJ, obtained by Equation (10), is needed, in addition to the EA and EI rigidities. The evaluation of the Poisson´s ratio, ν, is based on the bending, EI, and torsional, GJ, rigidities, and ν is independent of the value of t_n. The following expressions are used for assessment of G and ν [78]:

Preprints.org (www.preprints.org) | NOT PEER-REVIEWED | Posted: 9 April 2024 doi:10.20944/preprints202404.0629.v1

$$G = \frac{GJ}{2\pi t_n \left(\frac{EI}{EA}\right)\sqrt{8\left(\frac{EI}{EA}\right) - t_n^2}}, \quad (12)$$

$$\nu = \frac{E}{2G} - 1 = \frac{EI}{GJ} - 1. \quad (13)$$

Assuming the uncertainty of the values of the NT wall thickness, the surface Young's ($E_S = Et_n$) and shear ($G_S = Gt_n$) moduli, were calculated in the present study. In fact, the E_s and G_s elastic moduli are more reliable to describe the mechanical response of the nitride NTs, since they do not depend on the wall thickness. Considering that $t_n^2 \ll 8\left(\frac{EI}{EA}\right)$ and that the term t_n^2 in Equations (11) and (12) can be neglected, the surface Young´s, E_S, and shear, G_S, moduli are determined, respectively, as follows:

$$E_S = Et_n = \frac{EA}{\pi\sqrt{8\left(\frac{EI}{EA}\right)}}, \quad (14)$$

$$G_S = Gt_n = \frac{GJ}{2\pi\left(\frac{EI}{EA}\right)\sqrt{8\left(\frac{EI}{EA}\right)}}. \quad (15)$$

3. Results and Discussion: Elastic Properties of SWBNNTs, SWAlNNTs, SWGaNNTs, SWInNNTs and SWTlNNTs

3.1. Rigidities

The tensile, EA, bending, EI, and torsional, GJ, rigidities of the SWBNNTs, SWAlNNTs, SWGaNNTs, SWInNNTs and SWTlNNTs, calculated by Equations (8) – (10) from the FEA results, are plotted as a function of the nanotube diameter, D_n, in Figure 5a,c,e. For each of the rigidities EA, EI and GJ, the same trend is observed with the increase of the nanotube diameter, regardless of the NTs symmetry group (zigzag, chiral or armchair) and the nanotube compound. It is worth noting that the EA, EI and GJ rigidities decrease from the values obtained for SWBNNTs to those for SWTlNNTs. As previously established for the phosphide [79] and carbide [80,81] nanotubes, in the case of the 13th group element – nitride NTs, the tensile rigidity, EA, can be represented by a linear function of D_n (Figures 5a,b), while the bending, EI, and torsional, GJ, rigidities can be represented by a linear function of D_n^3 (Figure 5c,e and Figure 5d,f).

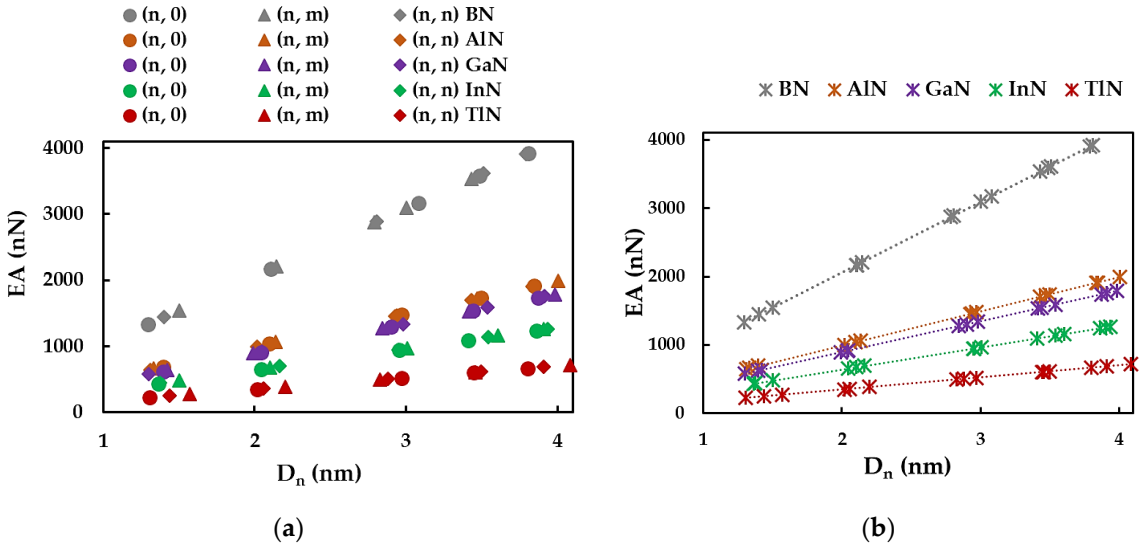

(a) (b)

Preprints.org (www.preprints.org) | NOT PEER-REVIEWED | Posted: 9 April 2024 doi:10.20944/preprints202404.0629.v1

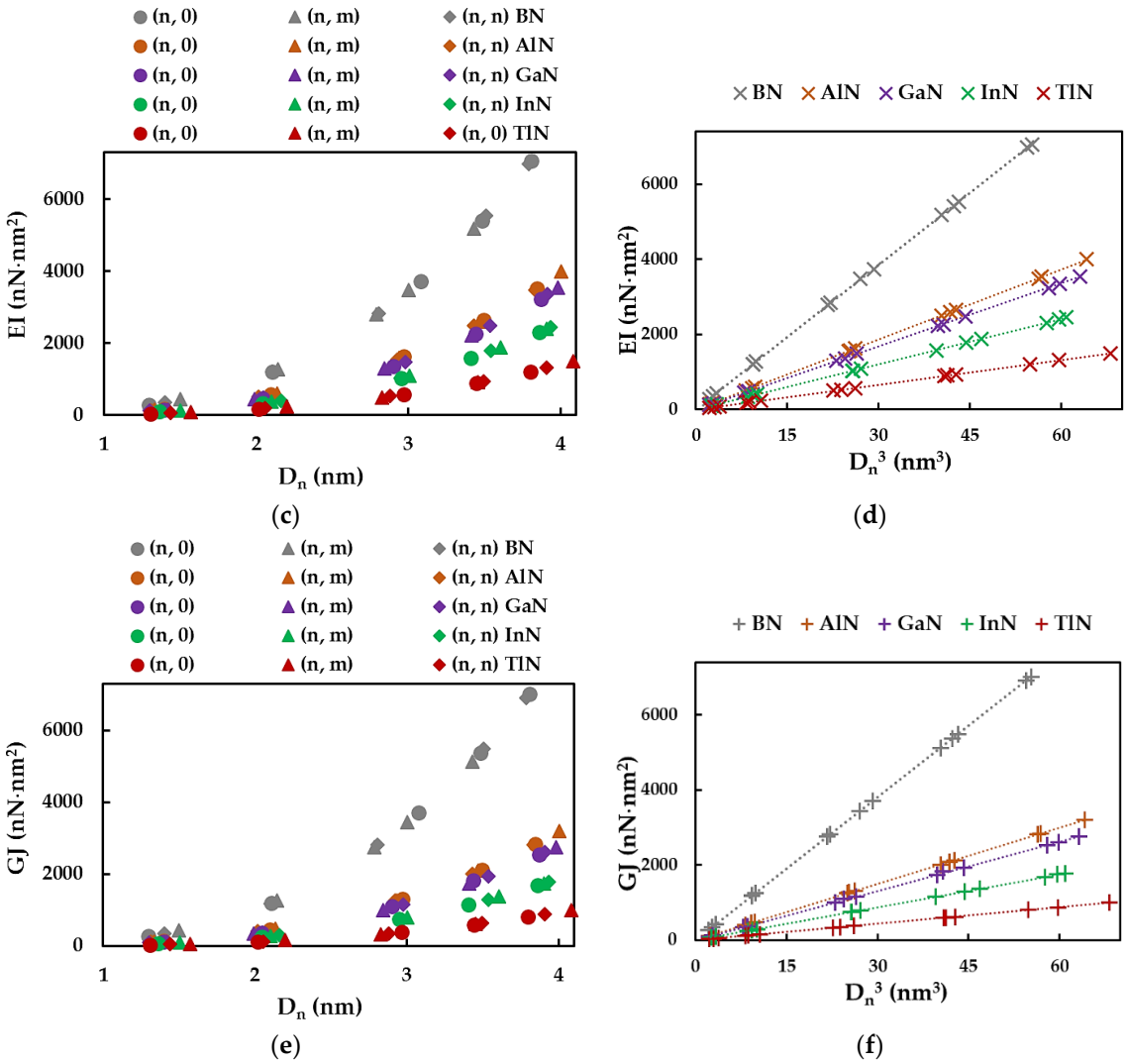

Figure 5. Evolutions of: (**a**,**b**) Tensile, EA, (**b**) Bending, EI, and (**c**) Torsional, GJ, rigidities as a function of the NT diameter, D_n, and (**d**) Bending, EI, and (**f**) Torsional, GJ, rigidities as a function of D_n^3, for the SWBNNTs, SWAlNNTs, SWGaNNTs, SWInNNTs and SWTlNNTs in Table 2.

Similar to what was found in the authors' previous work for the phosphide [79] and carbide [80,81] nanotubes, the slope of the straight lines in Figures 5b,d,f can be determined as follows:

$$EA = \alpha_{A13\text{-}N} D_n, \quad (16)$$

$$EI = \beta_{A13\text{-}N} D_n^{\,3}, \quad (17)$$

$$GJ = \gamma_{A13\text{-}N} D_n^{\,3}. \quad (18)$$

In these equations, $\alpha_{A13\text{-}N}$, $\beta_{A13\text{-}N}$ and $\gamma_{A13\text{-}N}$ are fitting parameters and D_n is the diameter of the nitride NTs. The values of these parameters, determined as slope of the dash lines in the graphs of Figures 5b,d,f, together with the mean differences between the values of EA, EI and GJ evaluated by the analytical expressions (16)–(18) and those derived from FEA (Equations (8)–(10)), are shown in Table 5. It can be seen in this table that the mean difference does not exceed 0.58%. Therefore, Equations (16)–(18) result in accurate values the three rigidities of SWBNNTs, SWAlNNTs, SWGaNNTs, SWInNNTs and SWTlNNTs, and can be used to evaluate the EA, EI and GJ rigidities without resource of numerical simulation.

Preprints.org (www.preprints.org) | NOT PEER-REVIEWED | Posted: 9 April 2024 doi:10.20944/preprints202404.0629.v1

Table 5. Fitting parameters $\alpha_{A13\text{-}N}$, $\beta_{A13\text{-}N}$ and $\gamma_{A13\text{-}N}$ for SWBNNTs, SWAlNNTs, SWGaNNTs, SWInNNTs and SWTlNNTs and mean difference between the EA, EI and GJ rigidities calculated with the aid of these parameters (Equations (16) – (18)) and the corresponding rigidities acquired from FEA.

Com-pound	Fitting parameters			Mean difference, %		
	$\alpha_{A13\text{-}N}$, nN/nm	$\beta_{A13\text{-}N}$, nN/nm	$\gamma_{A13\text{-}N}$, nN/nm	EA, nN	EI, nN·nm²	GJ, nN·nm²
BN	1029.96 [1]	128.08 [1]	126.93 [1]	0.08	0.23	0.08
AlN	497.38	62.09	49.94	0.23	0.36	0.31
GaN	448.92	55.99	43.78	0.24	0.34	0.58
InN	321.72 [1]	40.14 [1]	29.28 [1]	0.32	0.49	0.31
TlN	175.71	21.92	14.60	0.41	0.56	0.54

[1] Values of the fitting parameters for the BNNTs and InNNTs are similar to those obtained in the author's previous works [49,61].

The fitting parameters $\alpha_{A13\text{-}N}$, $\beta_{A13\text{-}N}$ and $\gamma_{A13\text{-}N}$ in Table 5 allow quantifying the tensile, EA, bending, EI, and torsional, GJ, rigidities, respectively, thereby describing the mechanical response of nanotubes under tension, bending and torsion. To this end, the values of $\alpha_{A13\text{-}N}$, and $\beta_{A13\text{-}N}$ together with $\gamma_{A13\text{-}N}$ are presented in Figure 6a,b, respectively, for the bond lengths, $a_{A13\text{-}N}$, corresponding to the SWBNNTs, SWAlNNTs, SWGaNNTs, SWInNNTs and SWTlNNTs. All three fitting parameters drop from SWBNNTs to SWAlNNTs, then the $\alpha_{A13\text{-}N}$, $\beta_{A13\text{-}N}$ and $\gamma_{A13\text{-}N}$ values decrease gradually, when moving to SWTlNNTs, i.e. as the $a_{A13\text{-}N}$ value increases (see Figure 6a,b). With regard to the relationship between bending, EI, and torsional, GJ, rigidities, which can be defined by the ratio between respective fitting parameters, $\beta_{A13\text{-}N}$ and $\gamma_{A13\text{-}N}$, the ratio $\beta_{A13\text{-}N}/\gamma_{A13\text{-}N} \approx 1$ for the SWBNNTs (see Figure 6c). It suggests that in this case, the EI and GJ rigidities are practically identical. For the remaining cases, the ratio of $\beta_{A13\text{-}N}/\gamma_{A13\text{-}N}$ becomes nearly equal to 1.2 for the SWAlNNTs, and continues increasing in increments of 0.1 up to $\beta_{A13\text{-}N}/\gamma_{A13\text{-}N} \approx 1.5$ for the SWTlNNTs. As seen in Figure 6c, increasing of the bond length, $a_{A13\text{-}N}$, leads to the decrease in torsional rigidity and, subsequently, to the more significant difference between the EI and GJ rigidities. It can be concluded that the SWInNNTs and SWTlNNTs with longer bond lengths, $a_{In\text{-}N} = 0.206$ nm and $a_{Tl\text{-}N} = 0.215$ nm, respectively, have weaker torsional properties when compared with those of the other 13th group atom –nitrides NTs.

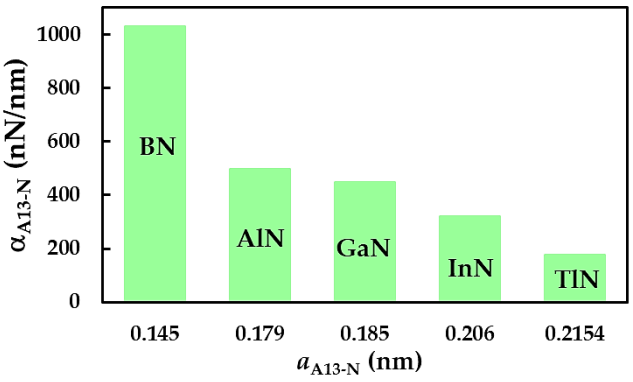

(a)

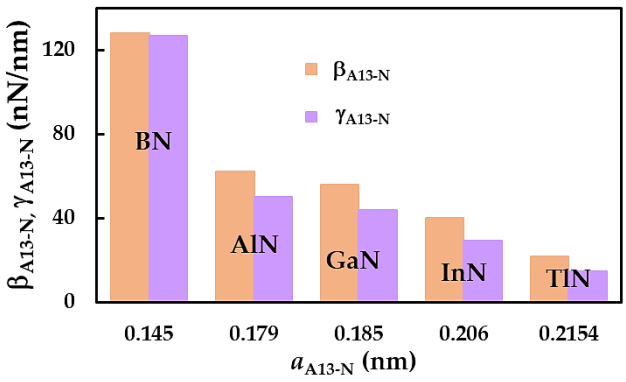

(b)

 doi:10.20944/preprints202404.0629.v1

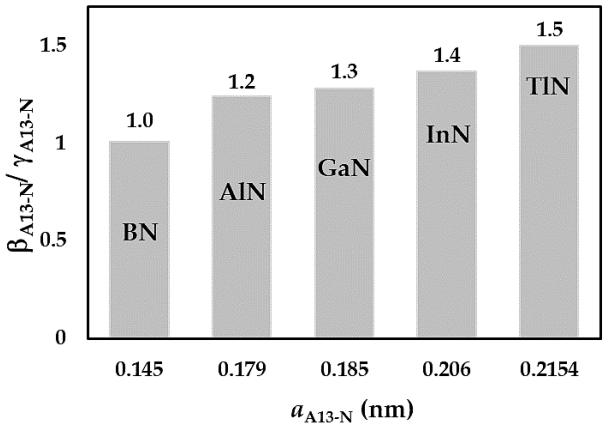

(**c**)

Figure 6. Fitting parameters as a function of the bond lengths, a_{A13-N}: (**a**) α_{A13-N}; (**b**) β_{A13-N} together with γ_{A13-N}, and (**c**) $\beta_{A13-N}/\gamma_{A13-N}$ ratio for SWBNNTs, SWAlNNTs, SWGaNNTs, SWInNNTs and SWTlNNTs.

3.2. Surface Young´s Modulus

The surface Young´s modulus, E_S, of the SWBNNTs, SWAlNNTs, SWGaNNTs, SWInNNTs and SWTlNNTs was assessed by Equation (14), which makes use of the results of the numerical tensile and bending tests. In addition, it is possible to obtain an analytical expression for E_S, which does not depend on D_n. For this, the tensile, EA, and bending, EI, rigidities in Equation (14) are replaced by expressions (16) and (17), leading to the following equation:

$$E_S = \frac{\alpha_{A13-N}}{\pi\sqrt{8\left(\frac{\beta_{A13-N}}{\alpha_{A13-N}}\right)}}. \quad (19)$$

where α_{A13-N} and β_{A13-N} are fitting parameters from Table 5.

Figure 7a shows the evolutions of the surface Young´s modulus, E_S, assessed by Equation (14) with the NT diameter, D_n, for all single-walled nitride nanotubes studied. The results of E_S calculated by Equation (19) are also plotted in Figure 7a, by dashed lines. For the 13th group – nitride NTs, regardless of the chiral angle (zigzag, chiral or armchair NTs) as well the compound (BN, AlN, GaN, InN or TlN), the surface Young's modulus is quasi-constant with increasing the NTs diameter, through the range of D_n considered in the current work. It can be concluded from Figure 7a that Equation (19) permits an accurate evaluation of the surface Young's modulus of nitride nanotubes. In fact, the mean differences between the values of E_S analytically evaluated by Equation (19) and those determined from the FEA with the aid of Equation (14) are 0.18%, 0.08%, 0.10%, 0.12% and 0.17% for the SWBNNTs, SWAlNNTs, SWGaNNTs, SWInNNTs and SWTlNNTs, respectively. As a result, the elastic properties of the nitride NTs can be accurately evaluated without resorting to numerical simulation. To examine the influence of the first element (B, Al, Ga, In, Tl) of nitride compound forming the nanotube on the E_S results, the values of the surface Young´s modulus, E_S, assessed by Equation (19) are plotted in Figure 7b, considering the respective bond lengths, a_{A13-N}.

Preprints.org (www.preprints.org) | NOT PEER-REVIEWED | Posted: 9 April 2024 doi:10.20944/preprints202404.0629.v1

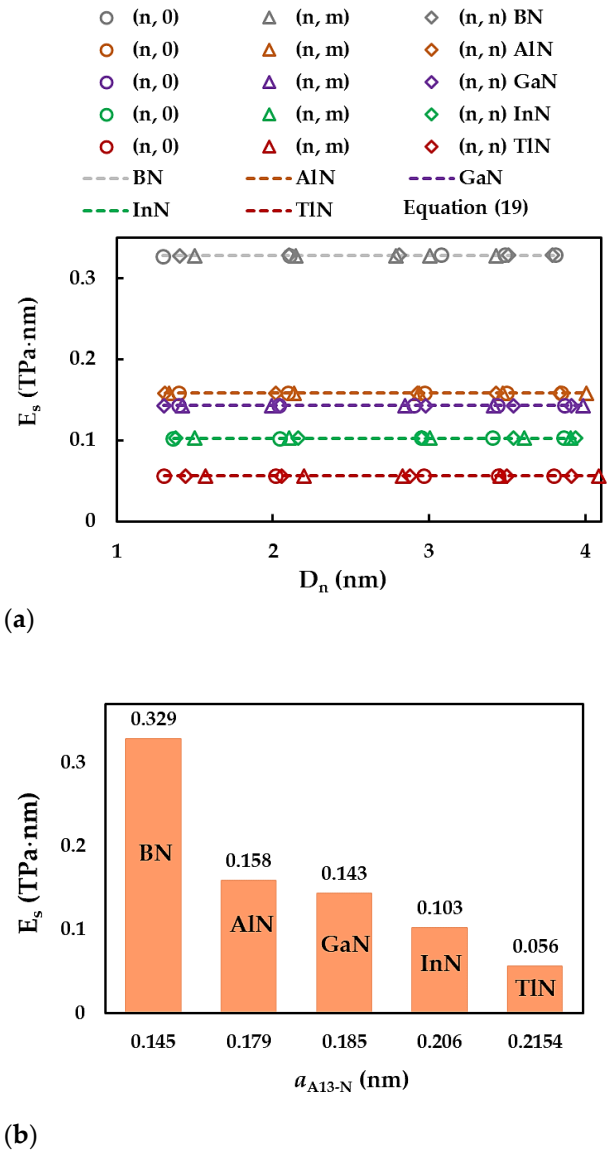

Figure 7. Evolutions of surface Young's modulus, E_S, for SWBNNTs, SWAlNNTs, SWGaNNTs, SWInNNTs and SWTlNNTs as a function of the: (**a**) NT diameter, D_n, and (**b**) bond lengths, $a_{A13\text{-}N}$.

The E_S value decreases by almost half when moving from SWBNNTs to SWAlNNTs, and E_S continues to decrease at a slower rate with increasing interatomic bond length, $a_{A13\text{-}N}$. The surface Young's modulus of SWTlNNTs ($a_{Tl\text{-}N}$ = 0.215 nm) is about 6 times lower when compared to that obtained for the SWBNNTs ($a_{B\text{-}N}$ = 0.145 nm). This decreasing trend of surface Young´s modulus with increasing bond length was also reported by Jiang and Guo [64], for nitride and phosphide NTs, and by Sakharova et al. [79], for phosphide NTs.

Figure 8 compares the surface Young´s modulus, E_S, values obtained for SWBNNTs (Figure 8a), and SWAlNNTs and SWGaNNTs (Figure 8b) with those available in the literature. Comprehensive comparison of the Young´s modulus results of SWBNNTs with literature was carried out in a previous work by the authors [49], and therefore only a few selected E_S values were currently chosen. The E_S results of Hao et al. [51], Kumar et al. [53], Santosh et al. [58], Oh [60], and Yan et al. [62], were calculated from the Young´s modulus, E, using the equality $E_S = Et_n$, for the NT wall thickness t_n = 0.333 nm [62], 0.340 nm [58], 0.330 nm [53,60] and 0.410 nm [51].

Preprints.org (www.preprints.org) | NOT PEER-REVIEWED | Posted: 9 April 2024 doi:10.20944/preprints202404.0629.v1

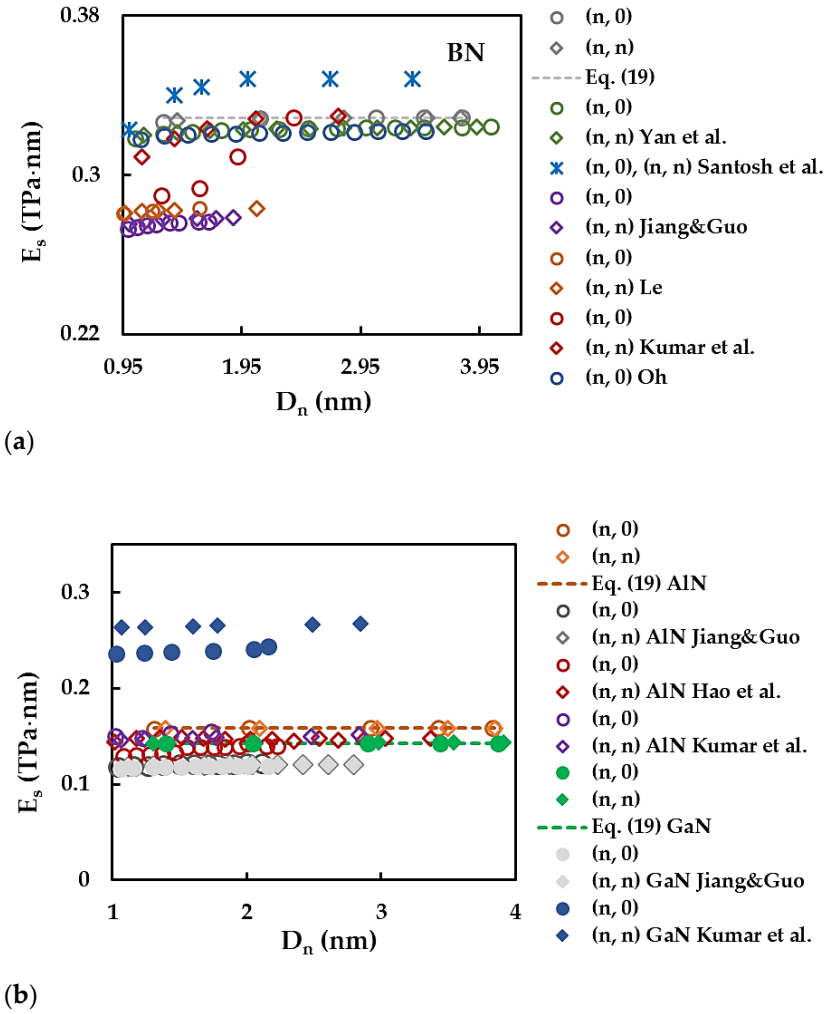

Figure 8. Comparison of the current evolutions of the surface Young's modulus, E_S, with those available in the literature, for: (**a**) SWBNNTs and (**b**) SWAlNNTs and SWGaNNTs, as a function of the NT diameter, D_n, [51,53,58–60,62,64].

A good agreement is observed when the current values of the SWBNNTs surface Young´s modulus are compared with those reported by Yan et al. [62] for non-chiral (zigzag and armchair) NTs (difference ≈ 1.30%), Oh [60] for zigzag NTs (difference ≈ 2.00%), and Kumar et al. [53] for armchair NTs with $D_n \gtrsim 1$ nm (difference ≈ 0.36%) and zigzag NTs with $D_n \gtrsim 1.95$ nm (difference ≈ 0.14%), as seen in Figure 8a. The E_S values of the SWAlNNTs evaluated in the present study are about 4.6% and 6.9% lower than those obtained in the works by Kumar et al. [53] and Hao et al. [51], respectively (Figure 8b). With regard to SWGaNNTs, a scattering of the surface Young´s modulus results is noticeable (see Figure 8b). Whatever the case, SWAlNNTs or SWGaNNTs, more Young´s modulus results are need to build a reliable benchmark to ascertain their elastic properties by theoretical methods.

3.3. Surface Shear Modulus and Poisson´s Ratio

In this section, two elastic properties are discussed that require torsional rigidity in addition to tensile and bending rigidities or just bending rigidity for their calculation, i.e. surface shear modulus and Poisson´s ratio, respectively.

The surface shear modulus, G_S, of the SWBNNTs, SWAlNNTs, SWGaNNTs, SWInNNTs and SWTlNNTs was evaluated by Equation (15), which makes use of the results of the numerical tensile, bending and torsional tests. Also, by replacing in Equation (15) the tensile, EA, bending, EI, and

 doi:10.20944/preprints202404.0629.v1

torsional, GJ, rigidities from expressions (16)–(18) and knowing the fitting parameters, $\alpha_{A13\text{-}N}$, $\beta_{A13\text{-}N}$ and $\gamma_{A13\text{-}N}$, from Table 5, G_S can be assessed analytically by the following expression:

$$G_S = \frac{\gamma_{A13\text{-}N}}{\pi\sqrt{32\left(\frac{\beta_{A13\text{-}N}}{\alpha_{A13\text{-}N}}\right)^3}}, \quad (20)$$

which allows calculating G_S without needing to know the NTs diameter, D_n.

The evolutions of the surface shear modulus, G_S, calculated by Equation (15) as a function of the NT diameter, D_n, together with the G_S values evaluated using Equation (20) are plotted in Figure 9a, for the cases of SWBNNTs, SWAlNNTs, SWGaNNTs, SWInNNTs and SWTlNNTs. For nitride nanotubes, whatever the NTs symmetry and the first element of nitride compound forming the NT, the surface shear modulus is quasi-constant with increasing of D_n. The mean differences between the G_S values calculated analytically by Equation (20) and those obtained from the FEA results with the help of Equation (15) are 0.13%, 0.17%, 0.59%, 0.19% and 0.26% (1.46%, 1.74%, 2.83%, 2.45% and 1.97% for NTs with $D_n \lesssim 1.5$ nm), for the SWBNNTs, SWAlNNTs, SWGaNNTs, SWInNNTs and SWTlNNTs, respectively. It can be concluded that Equation (20) allows an accurate evaluation of the surface shear modulus of the 13th group atom – nitride nanotubes, across the entire range of the NT diameters considered in the present study, although the error obtained for NTs with D_n up to 1.5 nm is slightly higher. The G_S values calculated by Equation (20) are shown in Figure 9b as a function of the bond length, $a_{A13\text{-}N}$.

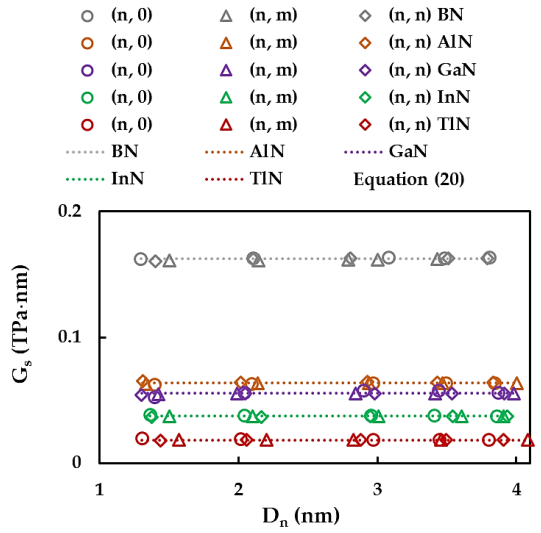

(**a**)

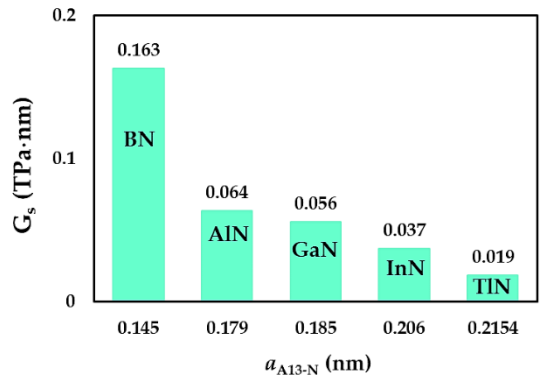

(**b**)

 doi:10.20944/preprints202404.0629.v1

Figure 9. Evolutions of the surface shear modulus, G_S, for SWBNNTs, SWAlNNTs, SWGaNNTs, SWInNNTs and SWTlNNTs as a function of the: (**a**) NT diameter, D_n, and (**b**) bond length, $a_{A13\text{-}N}$.

Similar to what was established for the surface Young´s modulus, the surface shear modulus, G_S, values decrease gradually with increasing the bond length, after an initial drop when moving from SWBNNTs to SWAlNNTs.

The G_S results available in the literature are scarce even for the case of SWBBNTs and show considerable discrepancy as seen in Figure 10a,b. Xiong and Tian [55], Kumar et al. [53], Santosh et al. [58] and Yan et al. [62] reported shear modulus, G, values. To enable a comparison, the respective surface shear modulus was calculated by using $G_S = Gt_n$ for the NT wall thickness t_n = 0.330 nm [53], 0.333 nm [62], 0.340 nm [58]. Xiong and Tian [55] did not report any t_n value, so in this case t_n = 0.34 nm [49] was used.

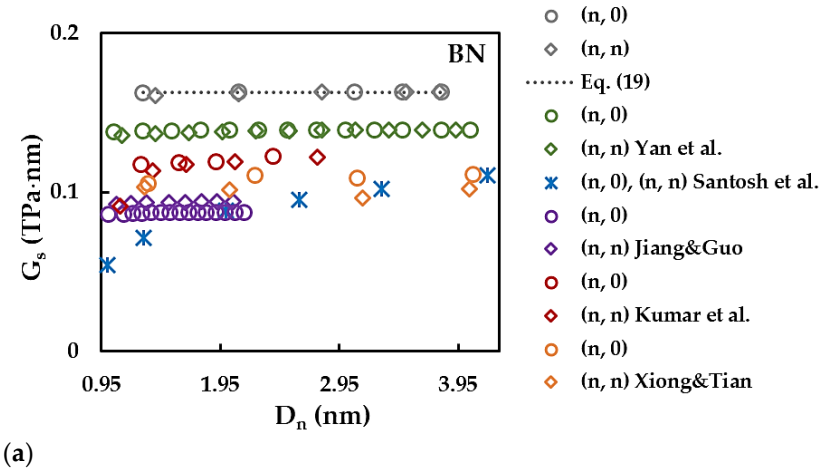

(**a**)

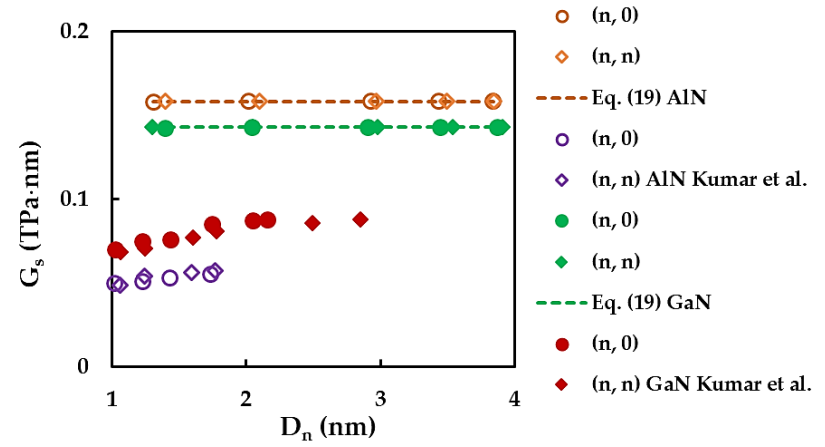

(**b**)

Figure 10. Comparison of the current evolutions of the surface shear modulus, G_S, with those available in the literature, for: (**a**) SWBNNTs and (**b**) SWAlNNTs and SWGaNNTs, as a function of the NT diameter, D_n, [53,55,58,62,68].

The Poisson's ratio, ν, of nitride nanotubes was assessed by Equation (13), using the EI and GJ rigidities, obtained from bending and torsional tests, respectively, and the $\beta_{A13\text{-}N}$ and $\gamma_{A13\text{-}N}$ fitting parameters in Table 5. This equation can be combined with expressions (17) and (18) for EI and GJ rigidities, to calculate ν, as follows:

Preprints.org (www.preprints.org) | NOT PEER-REVIEWED | Posted: 9 April 2024 doi:10.20944/preprints202404.0629.v1

$$\nu = \frac{\beta_{A13\text{-}N}}{\gamma_{A13\text{-}N}} - 1, \qquad (21)$$

whose expression is independent of the NT diameter.

Figure 11a shows the evolution of the Poisson's ratio, ν, calculated by Equation (13), with the NTs diameter, D_n, for the SWBNNTs, SWAlNNTs, SWGaNNTs, SWInNNTs and SWTlNNTs in Table 3. The values of ν calculated by Equation (21) are also presented in the Figure 11a. For zigzag, chiral and armchair nitride NTs with high value of D_n, the Poisson's ratio converges to the constant value calculated by Equation (21). The higher the value of the bond length, $a_{A13\text{-}N}$, the bigger the nanotube diameter, D_n^{st}, for which ν becomes stable (see Figure 11a). The D_n^{st} values are approximately 1.4 nm, 2.0 nm, 2.1 nm, 3.0 nm and 3,4 nm for SWBNNTs, SWAlNNTs, SWGaNNTs, SWInNNTs and SWTlNNTs, respectively. Similar qualitative results were reported for 13th group element - phosphide nanotubes [79]. For nitride NTs with diameter $D_n < D_n^{st}$, the Poisson's ratio increases for (n, 0) zigzag NTs, almost does not change for (n, m) chiral NTs and decreases for (n, n) armchair NTs.

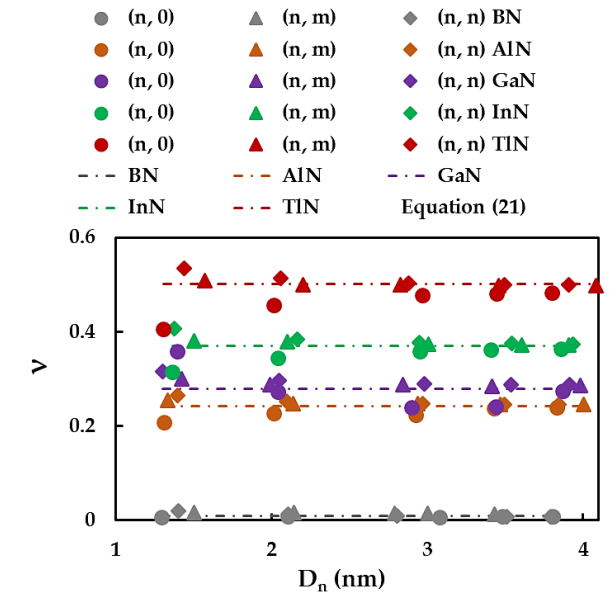

(**a**)

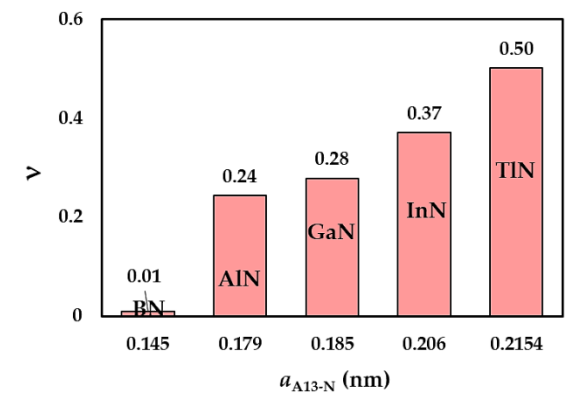

(**b**)

Figure 11. Evolutions of the Poisson's ratio, ν, for SWBNNTs, SWAlNNTs, SWGaNNTs, SWInNNTs and SWTlNNTs as a function of the: (**a**) NT diameter, D_n, and (**b**) bond length, $a_{A13\text{-}N}$.

Preprints.org (www.preprints.org) | NOT PEER-REVIEWED | Posted: 9 April 2024 doi:10.20944/preprints202404.0629.v1

To understand the effect of first element (B, Al, Ga, In, Tl) of nitride NTs on the Poisson´s ratio, the values of ν assessed by Equation (21) are shown in Figure 11b as a function of the bond length, $a_{A13\text{-}N}$. The lowest value of ν = 0.01 was found for SWBNNTs. The Poisson's ratio grows up to 0.24 when moving from SWBNNTs to SWAlNNTs, and then, ν continues to increase with increasing bond length. The highest ν value equal to 0.50 is observed for the SWTlNNTs, which value is about 50 times greater than that of SWBNNTs. This difference can be explained by the relationship between bending, and torsional rigidities, EI/GJ, necessary to determine ν by Equations (13) and (21). In fact, the $\beta_{A13\text{-}N}/\gamma_{A13\text{-}N}$ ratio is approximately equal to 1 and 1.5, for the SWBNNTs and SWTlNNTs, respectively. This means that bending, EI, and torsional, GJ, rigidities are almost the same for the boron nitride NTs and EI > GJ for the thallium nitride NTs, resulting in a substantial increase in the ν value of SWTlNNTs. The increase in Poisson´s ratio with increasing bond length was reported in the works by Jiang and Guo [64], for nitride and phosphide NTs, and by Sakharova et al. [79], for phosphide NTs.

Figure 12 compares the current Poisson´s ratio results with those available in the literature for the cases of SWBNNTs, SWAlNNTs and SWGaNNTs. A good agreement, with a difference of ≈ 2%, is found when the value of ν calculated by Equation (21) for SWGaNNTs is compared with that reported by Jiang and Guo [64] for the non-chiral GaN nanotubes. The Poisson´s ratios evaluated by Kumar et al. [53] for (n, 0) and (n, n) GaNNTs are ≈ 8% lower and ≈ 6% higher, respectively, than the ν values currently obtained. In other cases presented in Figure 12 there is considerable scattering of the ν values.

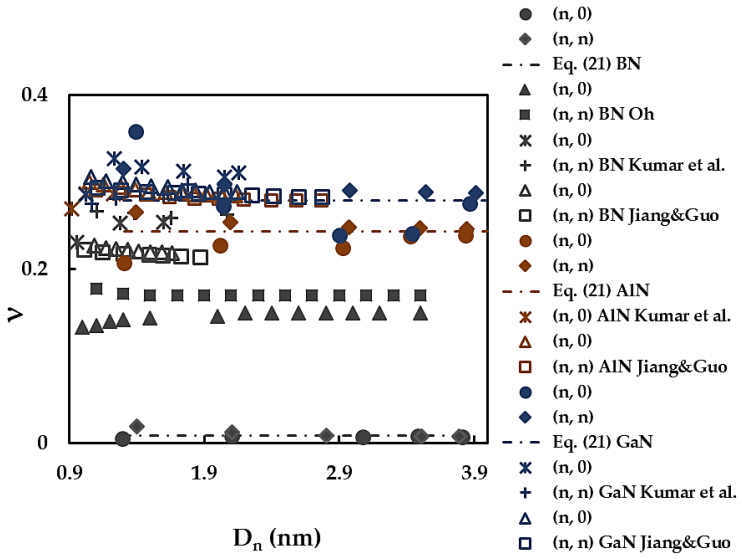

Figure 12. Comparison of the current evolutions of the Poisson´s ratio, ν, for SWBNNTs, SWAlNNTs and SWGaNNTs with those available in the literature, as a function of the NT diameter, D_n[53,60,64].

Jiang and Guo [64] reported for both armchair and zigzag SWBNNTs, SWAlNNTs and SWGaNNTs the trends in the evolutions of the Poisson's ratio as a function of NTs diameter, D_n, for which ν decreases with increasing D_n, and afterwards, the value of ν converges to an almost constant value (see Figure 12). This trend is in line with the current one for the evolutions of ν as a function of D_n, for armchair BN, AlN and GaN nanotubes, although, the decreasing rate found by Jiang and Guo [64] is slower.

4. Conclusions

The elastic properties, including the three rigidities, tensile, bending and torsional, the surface Young's and shear moduli and the Poisson´s ratio of SWBNNTs, SWAlNNTs, SWGaNNTs, SWInNNTs and SWTlNNTs, were evaluated in a numerical simulation study, based on the NCM/MSM approach. The main conclusions are specified below.

 doi:10.20944/preprints202404.0629.v1

Analytical expressions, which allow evaluating the three rigidities as a function of the NTs diameter and the fitting parameters without resorting to numerical simulation, were obtained for the most complete set of the 13th group atom - nitride nanotubes.

Also, the knowledge of these fitting parameters permits accurate analytical assessment of the surface Young´s and shear modulus of the SWBNNTs, SWAlNNTs, SWGaNNTs, SWInNNTs and SWTlNNTs with diameters, D_n, higher than 1.25 nm, and the Poisson's ratio, limiting to the nanotubes with diameters, $D_n > D_n^{st}$. The longer the bond length, the higher the value of D_n^{st}, for which the Poisson´s ratio does not change with the increase in the NT diameter.

The tensile, bending and torsional rigidities, the surface Young's and shear moduli, and the Poisson´s ratio of SWBNNTs, SWAlNNTs, SWGaNNTs, SWInNNTs and SWTlNNTs are sensitive to the interatomic bond length of the hexagonal lattice. The three rigidities, and the surface Young´s and shear moduli decrease, while the Poisson´s ratio increases, with increasing bond length.

The results presented constitute a considerable contribution to a benchmark about the determination of the elastic properties of nitride nanotubes by theoretical methods.

Author Contributions: Conceptualization, N.A.S., A.F.G.P., J.M.A. and J.V.F.; methodology, N.A.S., A.F.G.P. and J.M.A.; investigation, N.A.S. and A.F.G.P.; software, B.M.C. with support of J.M.A.; formal analysis, N.A.S., A.F.G.P., J.M.A., T.G.P., J.V.F. and; writing - original manuscript, N.A.S. and J.V.F.; writing - review and editing, all the authors. All authors have read and agreed to the published version of the manuscript.

Funding: This research is sponsored by FEDER funds through the program COMPETE—Programa Operacional Factores de Competitividade—and by national funds through FCT, Fundação para a Ciência e a Tecnologia, under the projects CEMMPRE - UIDB/00285/2020 and ARISE - LA/P/0112/2020

Informed Consent Statement: Not applicable.

Data Availability Statement: The data presented in this study are available on request from the corresponding author after obtaining permission of authorized person.

Conflicts of Interest: The authors declare no conflict of interest. The funders had no role in the design of the study; in the collection, analyses, or interpretation of data; in the writing of the manuscript, or in the decision to publish the results.

References

1. Ye, C.; Peng, Q. Mechanical Stabilities and Properties of Graphene-like 2D III-Nitrides: A Review. *Crystals* **2023**, *13*, 12
2. Zheng, F.; Xiao, X.; Xie, J.; Zhou, L.; Li, Y.; Dong, H. Structures, properties and applications of two-dimensional metal nitrides: from nitride MXene to other metal nitrides. *2D Mater.* **2022**, *9*, 022001
3. Abdullah, N.R..; Abdullah, B.J.; Gudmundsson, V. Electronic and optical properties of metallic nitride: A comparative study between the MN (M = Al, Ga, In, Tl) monolayers. *Solid State Commun.* **2022**, *346*, 114705
4. Elahi, S.M.; Farzan, M.; Salehi, H.; Abolhasani, M.R. An investigation of electronic and optical properties of TlN nanosheet and compare with TlN bulk (Wurtzite) by first principle. *Optik* **2016**, *127*, 9367 – 9376
5. Golberg, D.; Bando, Y.; Huang, Y.; Terao, T.; Mitome, M.; Tang, C.; Zhi, C. Boron nitride nanotubes and nanosheets. *ACS Nano* **2010**, *4*, 2979 – 2993
6. Wang, Y.; Zhou, V.; Xie Y.; Zheng, X.-Q.; Feng, P.X.-L. Optical contrast signatures of hexagonal boron nitride on a device platform. *Opt. Mater. Express.* **2019**, *9*, 1223 – 1232
7. Song, L.; Ci, L.; Lu, H.; Sorokin, P.B.; Jin, C.; Ni, J.; Kvashnin, A.G.; Kvashnin, D.G.; Lou, J.; Yakobson, B.I.; Ajayan, P.M. Large scale growth and characterization of atomic hexagonal boron nitride layers. *Nano Lett.* **2010**, *10*, 3209 – 3215
8. Vurgaftman, I.; Meyer, J.R. Band parameters for nitrogen-containing semiconductors. *J. Appl. Phys.* **2003**, *94*, 3675 – 3696
9. Chattopadhyay, S.; Ganguly, A.; Chen, K.-H.; Chen, L.-Ch. One-Dimensional Group III-Nitrides: Growth, Properties, and Applications in Nanosensing and Nano-Optoelectronics. *Crit. Rev. Solid State Mater. Sci.* **2009**, *34*, 224 — 279
10. Zaoui, A. Plane wave pseudopotential study of ground state properties and electrochemical description of thallium nitride. *Mater. Sci. Eng.B* **2003**, *103*, 258 – 261
11. Li-Wei, S.; Yi-Feng, D.; Li-Xia, Q. Structural Stability and Elastic Properties of Wurtzite TlN under Hydrostatic Pressure. *Chin. Phys. Lett.* **2010**, *27*, 080505

 doi:10.20944/preprints202404.0629.v1

12. Walker, K.E.; Rance, G.A.; Pekker, A.; Tóháti, H.M.; Fay, M.W.; Lodge, R.W.; Stoppiello, C.T.; Kamarás, K.; Khlobystov, A.N. Growth of carbon nanotubes inside boron nitride nanotubes by coalescence of fullerenes: toward the world's smallest coaxial cable. *Small Methods* **2017**, *1*, 1700184
13. Huang, Z.; Lü, T.-Y.; Wang, H.-Q.; Yang, S.-W.; Zheng, J.-C. Electronic and thermoelectric properties of the group-III nitrides (BN, AlN and GaN) atomic sheets under biaxial strains. *Comput. Mater. Sci.* **2017**, *130*, 232 – 241
14. Amorim, B.; Cortijo, A.; de Juan, F.; Grushin, A.G.; Guinea, F.; Gutiérrez-Rubio, A.; Ochoa, H.; Parente, V.; Roldán, R.; San-José, P.; Schiefele, J.; Sturla, M.; Vozmediano, M.A.H. Novel effects of strains in graphene and other two dimensional materials. *Phys. Rep.* **2016**, *617*, 1 – 54
15. Behzad, S. Effects of strain and thickness on the electronic and optical behaviors of two-dimensional hexagonal gallium nitride. *Superlattices Microstruct.* **2017**, *106*, 102–110
16. Liu, P.; Sarkar, A.D.; Ahuja, R. Shear strain induced indirect to direct transition in band gap in AlN monolayer nanosheet. *Comput. Mater. Sci.* **2014**, *86*, 206–210
17. Beshkova, M.; Yakimova R. Properties and potential applications of two-dimensional AlN. *Vacuum* **2020**, *176*, 109231
18. Chowdhury, R.; Adhikari, S. Boron-nitride nanotubes as zeptogram-scale bionanosensors: Theoretical investigations. *IEEE Trans. Nanotechnol.* **2011**, *10*, 659 – 667
19. Noei, M.; Soleymanabadi, H.; Peyghan, A.A. Aluminum nitride nanotubes. *Chem. Pap.* **2017**, *71*, 881–893
20. Albarakati, R.; Al-Qurashi, O.; Safi, Z.; Wazzan, N.A dispersion-corrected DFT calculation on encapsulation of favipiravir drug used as antiviral against COVID-19 into carbon-, boron-, and aluminum-nitride nanotubes for optimal drug delivery systems combined with molecular docking simulations. *Struct Chem.* **2023**, *11*, 1–19
21. Liu, B.; Bando, Y.; Wang, M.; Tang, C.; Mitome, M.; Golberg, D. Crystallography and elasticity of individual GaN nanotubes, *Nanotechnology* **2009**, *20*, 185705
22. Rubio, A.; Corkill, J.; Cohen, M.L. Theory of graphitic boron nitride nanotubes. *Phys. Rev. B* **1994**, *49*, 5081 – 5084
23. Chowdhury, R.; Adhikari, S. Boron-nitride nanotubes as zeptogram-scale bionanosensors: Theoretical investigations. *IEEE Trans. Nanotechnol.* **2011**, *10*, 659 – 667
24. Lourie, O.R.; Jones, C.R.; Bartlett, B.M.; Gibbons, P.C.; Ruoff, R.S.; Buhro, W.E. CVD growth of boron nitride nanotubes. *Chem. Mater.* **2000**, *12*, 1808 – 1810
25. Ahmad, P.; Khandaker, M.U.; Khana, Z.R. Amina, Y.M. Synthesis of boron nitride nanotubes via chemical vapour deposition: a comprehensive review. *RSC Adv.* **2015**, *5*, 35116 – 35137
26. Kim, J.; Lee, S.; Uhm, Y.R.; Jun, J.; Rhee, C.K.; Kim, G.M. Synthesis and growth of boron nitride nanotubes by a ball milling–annealing process. *Acta Mater.* **2011**, *59*, 2807 – 2813
27. Golberg, D.; Bando, Y.; Eremets, M.; Takemura, K.; Kurashima, K.; Yusa, H. Nanotubes in boron nitride laser heated at high pressure. *Appl. Phys. Lett.* **1996**, *69*, 2045 – 2047
28. Kim, K.S.; Couillard, M.; Shin, H.; Plunkett, M.; Ruth, D.; Kingston, C.T.; Simard, B. Role of hydrogen in high-yield growth of boron nitride nanotubes at atmospheric pressure by induction thermal plasma. *ACS Nano* **2018**, *12*, 884 – 893
29. Zhang, D.; Zhang, R. Theoretical prediction on aluminum nitride nanotubes. *Chem. Phys. Lett.* **2003**, *371*, 426–432
30. Wu, Q.; Hu, Z.; Wang, X.; Lu, Y.; Chen, X.; Xu, H.; Chen, Y. Synthesis and characterization of faceted hexagonal aluminum nitride nanotubes. *J. Am. Chem. Soc.* **2003**, *125*, 10176 – 10177
31. Balasubramanian, C.; Bellucci, S.; Castrucci, P.; De Crescenzi M.; Bhoraskar S. () Scanning tunneling microscopy observation of coiled aluminum nitride nanotubes *Chem. Phys. Lett.* **2004**, *383*, 188–191
32. Yin, L.W.; Bando, Y.; Zhu, Y.C.; Li, M.S.; Tang, C.-C.; Golberg, D. Single-crystalline AlN nanotubes with carbon-layer coatings on the outer and inner surfaces via a multiwalled-carbon-nanotubetemplate-induced route. *Adv. Mater.* **2005**, *17*, 213–217
33. Stan, G.; Ciobanu, C.V.; Thayer, T.P.; Wang, G.T.; Creighton, J.R.; Purushotham, K.P.; Bendersky, L.A.; Cook, R.F. Elastic moduli of faceted aluminum nitride nanotubes measured by contact resonance atomic force microscopy. *Nanotechnology* **2009**, *20*, 035706
34. Fan, Y. Formation of crystalline AlN nanotubes by a roll-up approach. *Mater. Lett.* **2011**, *65*, 1900 – 1902
35. Lee, S.M.; Lee, Y.H.; Hwang, Y.G.; Elsner, J.; Porezag, D.; Frauenheim, T. Stability and electronic structure of GaN nanotubes from density-functional calculations. *Phys. Rev. B* **1999**, *60*, 7788 – 7791
36. Goldberger, J.; He, R.; Zhang, Y.; Lee, S.; Yan, H.; Choi, H.-J.; Peidong, Y. Single-crystal gallium nitride nanotubes. *Nature* **2003**, *422*, 599 – 602
37. Yin, L.W.; Bando, Y.; Zhu, Y.C.; Golberg, D.; Yin, L.W.; Li, M.S. Indium-assisted synthesis on GaN nanotubes. *Appl. Phys. Lett.* **2004**, *84*, 3912–3914
38. Hu, J.Q.; Bando, Y.; Golberg, D.; Liu, Q.L. Gallium Nitride Nanotubes by the Conversion of Gallium Oxide Nanotubes. *Angew. Chem. Int. Ed.* **2003**, *42*, 3493 – 3497

 doi:10.20944/preprints202404.0629.v1

39. Hung, S.-C.; Su, Y.-K.; Fang, T.-H.; Chang, S.-J.; Ji, L-W. Buckling instabilities in GaN nanotubes under uniaxial compression. *Nanotechnology* **2005**, *16*, 2203 – 2208
40. Liu, B.D.; Bando, Y.; Tang, C.C.; Shen, G.Z.; Golberg, D.; Xu, F.F. Wurtzite-type faceted single-crystalline GaN nanotubes. *Appl. Phys. Lett.* **2006**, *88*, 093120
41. Jung, W.-G.; Jung, S.-H.; Kung, P.; Razeghi, M. Fabrication of GaN nanotubular material using MOCVD with an aluminium oxide membrane. *Nanotechnology* **2006**, *17*, 54–59
42. Yin, L.; Bando, Y.; Golberg, D.; Li, M. Growth of single-crystal indium nitride nanotubes and nanowires by controlled-carbonitridation reaction route. *Adv. Mater.* **2004**, *16*, 1833 – 1838
43. Sardar, K.; Deepak, F.L.; Govindaraj, A.; Seikh, M.M.; Rao, C.N.R. InN nanocrystals, nanowires, and nanotubes. *Small* **2005**, *1*, 91 – 94
44. Qian, Z.; Hou, S.; Zhang, J.; Li, R.; Shen, Z.; Zhao, X.; Xue, Z. Stability and electronic structure of single-walled InN nanotubes. *Physica E* **2005**, *30*, 81 – 85
45. Shah, E.V.; Roy, D.R. Density functional investigation on hexagonal nanosheets and bulk thallium nitrides for possible thermoelectric applications. *Appl. Nanosci*. **2019**, *9*, 33–42
46. Li, X.; Dai, Y.; Ma, Y.; Wei, W.; Yu, L.; Huang, B. Prediction of large-gap quantum spin hall insulator and Rashba-Dresselhaus effect in two-dimensional g-TlA (A = N, P, As, and Sb) monolayer films. *Nano Res.* **2015**, *8*, 2954–2962
47. Peng, Q.; Liang, C.; Ji, W.; De, S. A First Principles Investigation of the Mechanical Properties of *g*-TlN. *Modeling and Numerical Simulation of Material Science (MNSMS)* **2012**, *2*, 76–84
48. Antunes, J.M.; Pereira, A.F.G.; Sakharova, N.A. Overview on the Evaluation of the Elastic Properties of Non-Carbon Nanotubes by Theoretical Approaches. *Materials* **2022**, *15*, 3325
49. Sakharova, N.A.; Antunes, J.M.; Pereira, A.F.G.; Chaparro, B.M.; Fernandes, J.V. On the determination of elastic properties of single-walled boron nitride nanotubes by numerical simulation. *Materials* **2021**, *14*, 3183
50. Kochaev, A. Elastic properties of noncarbon nanotubes as compared to carbon nanotubes. *Phys. Rev. B* **2017**, *96*, 155428
51. Hao, J.-H.; Wang, Y.-F.; Yin, Y.-H.; Jiang, R.; Wang, Y.-F.; Jin, Q.-H. An ab initio study of the size-dependent mechanical behavior of single-walled AlN nanotubes, *Solid State Sci.* **2015**, *45*, 30 – 34
52. Fabris, G.S.L.; Paskocimas, C.A.; Sambrano, J.R.; Paupitz, R. One- and two-dimensional structures based on gallium nitride. *J. Solid State Chem.* **2021**, *303*, 122513
53. Kumar, D.; Verma, V.; Dharamvir, K.; Bhatti, H.S. Elastic moduli of boron nitride, aluminium nitride and gallium nitride nanotubes using second generation reactive empirical bond order potential. *Multidiscip. Model. Mater. Struct.* **2015**, *11*, 2 – 15
54. Jeng, Y.-R.; Tsai, P.C.; Fang, T.-H. Molecular dynamics investigation of the mechanical properties of gallium nitride nanotubes under tension and fatigue. *Nanotechnology* **2004**, *15*, 1737 – 1744
55. Xiong, Q.-lin.; Tian, X.G. Torsional properties of hexagonal boron nitride nanotubes, carbon nanotubes and their hybrid structures: A molecular dynamics study. *AIP Adv.* **2015**, *5*, 107215
56. Tao, J.; Xu, G.; Sun, Y. Elastic properties of boron-nitride nanotubes through an atomic simulation method. *Math. Prob. Eng.* **2015**, 240547
57. Xu, B.; J. Lu, A.; Pan, B.C.; Yu, Q.X. Atomic structures and mechanical properties of single-crystal GaN nanotubes, *Phys. Rev. B* **2005**, *71*, 125434
58. Santosh, M.; Maiti, P.K.; Sood, A.K. Elastic properties of boron nitride nanotubes and their comparison with carbon nanotubes. *J. Nanosci. Nanotech.* **2009**, *9*, 1 – 6
59. Le, M.-Q. Young's modulus prediction of hexagonal nanosheets and nanotubes based on dimensional analysis and atomistic simulations. *Meccanica* **2014,** *49*, 1709 – 1719
60. Oh, E.-S. Elastic properties of boron-nitride nanotubes through the continuum lattice approach. *Mater. Lett.* **2010**, *64*, 859 – 862
61. Sakharova, N.A.; Pereira, A.F.G.; Antunes, J.M.; Chaparro, B.M.; Fernandes, J.V. On the determination of elastic properties of indium nitride nanosheets and nanotubes by numerical simulation. Metals **2023**, *13*, 73
62. Yan, J.W.; He, J.B.; Tong. L.H. Longitudinal and torsional vibration characteristics of boron nitride nanotubes. *J. Vib. Eng. Technol.* **2019,** *7*, 205 – 215
63. Genoese, A.; Genoese A.; Salerno, G. On the nanoscale behaviour of single-wall C, BN and SiC nanotubes. *Acta Mech.* **2019**, *230*, 1105 – 1128
64. Jiang, L.; Guo, W. Analytical solutions for elastic binary nanotubes of arbitrary chirality. *Acta Mech. Sin.* **2016,** *32*, 1046 – 1057
65. Şahin, H.; Cahangirov, S.; Topsakal, M.; Bekaroglu, E.; Akturk, E.; Senger, R.T.; Ciraci, S. Monolayer honeycomb structures of group-IV elements and III-V binary compounds: First-principles calculations. *Phys. Rev. B* **2009**, *80*, 155453
66. Tapia, A.; Cab, C.; Hernández-Pérez, A.; Villanueva, C.; Peñuñuri, F.; Avilés, F. The bond force constants and elastic properties of boron nitride nanosheets and nanoribbons using a hierarchical modeling approach. *Physica E* **2017**, *89*, 183 – 193

 doi:10.20944/preprints202404.0629.v1

67. Menon, M.; Srivastava, D. Structure of boron nitride nanotubes: tube closing versus chirality. *Chem. Phys. Lett.* **1999**, *307*, 407 – 412
68. Jiang, L.; Guo, W. A molecular mechanics study on size-dependent elastic properties of single-walled boron nitride nanotubes. *J. Mech. Phys. Solids* **2011**, *59*, 1204 – 1213
69. Kang, J.W.; Hwang, H.J. Atomistic study of III-nitride nanotubes. *Comput. Mater. Sci.* **2004**, *31*, 237 – 246
70. Huber, K.P., Hertzberg, G. *Molecular Spectra and Molecular Siructure: IV. Constants of Diatomic Molecules*, 1st ed.; Van Nostrand Reinhold Company: New York, USA, 1979
71. Zhou, Z.; Zhao, J.; Chen, Y.; Schleyer, Pv.R.; Chen, Z. Energetics and electronic structures of AlN nanotubes/wires and their potential application as ammonia sensors. *Nanotechnology* **2007**, *18*, 42402
72. Lee, S.M.; Lee, Y.H.; Hwang, Y.G.; Elsner, J.; Porezag, D.; Frauenheim, T. Stability and electronic structure of GaN nanotubes from density-functional calculations. *Phys. Rev. B* **1999**, *60*, 7788
73. Li, C.; Chou, T.W. A structural mechanics approach for the analysis of carbon nanotubes. *Int. J. Solids Struct.* **2003**, *40*, 2487 – 2499
74. Genoese, A.; Genoese, A.; Rizzi, N. L.; Salerno, G. Force constants of BN, SiC, AlN and GaN sheets through discrete homogenization. *Meccanica* **2018**, *53*, 593 – 611
75. Ansari, R.; Rouhi, S.; Mirnezhad, M.; Aryayi, M. Stability characteristics of single-walled boron nitride nanotubes. *Arch. Civ. Mech. Eng.* **2015**, *15*, 162 – 170
76. Mayo, S.L.; Barry D. Olafson, B.D.; Goddard, W.A. DREIDING: A generic force field for molecular simulations. *J. Phys. Chem.* **1990**, *94*, 8897 – 8909
77. Sakharova, N.A.; Pereira, A.F.G.; Antunes, J.M.; Brett, C.M.A.; Fernandes. J.V. Mechanical characterization of single-walled carbon nanotubes. Numerical simulation study. *Compos. B-Eng*. **2015,** *75*, 73 – 85
78. Pereira, A.F.G.; Antunes, J.M.; Fernandes. J.V.; Sakharova, N.A. Shear modulus and Poisson's ratio of single-walled carbon nanotubes: numerical evaluation. *Phys. Status Solidi B* **2016**, *253*, 366 – 376
79. Sakharova, N.A.; Antunes, J.M.; Pereira, A.F.G.; Chaparro, B.M.; Fernandes, J.V. Elastic properties of single-walled phosphide nanotubes: Numerical Simulation Study. *Nanomaterials* **2022**, *12*, 2360
80. Sakharova, N.A.; Pereira, A.F.G.; Antunes, J.M. Elastic moduli of non-chiral singe-walled silicon carbide nanotubes: numerical simulation study. *Materials* **2022**, *15*, 8153
81. Fernandes, J.V.; Pereira, A.F.G.; Antunes, J.M.; Chaparro, B.M.; Sakharova, N.A. Numerical Simulation Study of the Mechanical Behaviour of 1D and 2D Germanium Carbide and Tin Carbide Nanostructures. *Materials* **2023**, *16*, 5484